Updated inundation modelling in Canterbury from a South American tsunami

Prepared for Environment Canterbury

Environment Canterbury report number R14/78

November 2014

Authors/Contributors:
Emily Lane
Alison Kohout
Antoine Chiaverini
Jade Arnold

For any information regarding this report please contact:

Emily Lane
Coastal Hazards Modeller
Hydrodynamics
+64-3-348 8987
Emily.Lane@niwa.co.nz

National Institute of Water & Atmospheric Research Ltd
10 Kyle Street
Riccarton
Christchurch 8011

Phone +64 3 348 8987

Contents

Figures

Reviewed by   Approved for release by

David Plew   Charles Pearson

Executive summary

- NIWA was commissioned to undertake a numerical tsunami modelling study of inundation resulting from a M_w 9.485 earthquake originating in the subduction zone off Peru across the Pacific ocean. The areas of focus are Kaikoura and surrounds, Pegasus Bay, including Christchurch, Lyttelton and Akaroa Harbours and South Canterbury. These are the areas modelled for a smaller scenario in previous reports (Gillibrand, Arnold et al. 2011; Lane, Arnold et al. 2012; Lane and Arnold 2013).

- The choice of scenario was based on the 2013 Tsunami Review (Power 2013a). Deaggregation of the source of tsunami representing the 2500 year return period at the 84 percentile confidence interval (1 standard deviation above mean) in the Christchurch region identified South Peru / North Chile as a major source of the hazard. M_w 9.485 was a magnitude of earthquake needed from this location to give the 2,500 return period wave heights at the Christchurch coast.

- We assumed that the largest wave arrival coincides with Mean High Water Spring (MHWS).

- Water elevations for the Canterbury coast were 4 to over 10 m above the quiescent water level, with the larger values being in Pegasus Bay and around Banks Peninsula.

- Kaikoura township and South Bay, Motunau and Waikuku Beach, Kairaki, the Pines, Brooklands, Spencerville, New Brighton, Bexley, South Shore, Ferrymead, McCormacks Bay, Redcliffs, Moncks Bay, Sumner, Taylors Mistake, Lyttelton Port, Teddington and low lying land in Lyttelton Harbour, Akaroa township and low lying land in Akaroa Harbour and Timaru port were inundated. The worst inundation was around Christchurch. Beyond these areas, land inundation was generally confined to river mouths and the coastal strip.

- Maximum flow speeds were 2-3 m/s in most places. They exceeded 5 m/s at some river mouths, especially in Pegasus Bay. Flow speeds tended to be lower in the Kaikoura region.

- Arrival times of the first wave are between 14 to 15 hours after fault rupture but the largest wave generally arrives between 17-20 hours after fault rupture. Significant wave arrivals can also occur between 21-25 hours after fault rupture. There is often a chain of large waves and significant disturbances continue for at least 24 hours after the first wave arrival, gradually decreasing in strength.

Use of this report

The main purpose of this report is to help inform evacuation planning and emergency management planning. The scenario modelled has a high return period in the order of 2500 years and represents an extreme scenario, which is appropriate for evacuation planning and emergency management planning. The report is not intended to be used for land use planning, because land use planning generally uses shorter return periods of up to 500 years – the inundation from a 500 year return period tsunami may be considerably less than shown in this report. However, the information in the report may be useful for strategic development planning and infrastructure planning as it may, used with other hazard information, highlight areas of higher vulnerability where future development

should be more carefully managed. The spatial data in these layers have been generated at a scale of 1:25,000 and should not be used at scales finer than this.

Caveat

This report is based on state-of-the-art knowledge and modelling capabilities of tsunamis and tsunami inundation. While every effort is made to provide accurate information, there are many uncertainties involved including knowledge of potential tsunami sources, source characteristics, bathymetry and topography. In addition, while the hydrodynamic model, RiCOM, captures much of the physics involved in tsunami propagation and inundation, it also includes some simplifying assumptions as with all models. The information provided in this report is of a technical nature and should be considered with the above limitations in mind.

1   Introduction

The Canterbury coast lies on the western edge of the Pacific Ocean and is subject to local, regional and distant-source tsunamis. In historical times several large tsunamis that originated in South America have significantly impacted the Canterbury coast including in 1868, 1877 and 1960. In the 2013 Tsunami Review (Power 2013a) a probabilistic tsunami hazard assessment (PTHA) of the tsunami wave height at coast was undertaken for all of New Zealand. This PTHA estimates the maximum wave height at the New Zealand coast for return periods of 500 and 2,500 years. The assessment gives a distribution of possible maximum wave heights for different confidence levels, which takes into account uncertainty in the source parameters used in the assessment. GNS Science recommends using the wave height at the coast representing the 2500 year return period at the 84 percentile confidence interval (1 standard deviation above mean) for evacuation planning. This value for Christchurch was given in (Power 2013a) as 12.63 m. The deaggregation of this wave height identified South Peru / North Chile as a major source of the hazard and that an earthquake of magnitude M_w 9.485 was required to give that wave height at the Christchurch coast (Power 2014, pers. comm.). This compares with an expected wave height of 9.64 m for the 2,500 year return period at the 50th percentile which corresponds to an earthquake of magnitude M_w 9.41 (Power 2013b). Similar results held for most of the Canterbury coast with earthquakes of magnitude ranging between M_w 9.4 and 9.5. The only exception to this was the Kaikoura coast which required an earthquake of M_w 9.57 – 9.74 from Peru to reach its expected 2,500 year 84th percentile tsunami hazard. This higher magnitude required partially reflects the fact that the Kaikoura coast is less exposed to tsunamis from Peru than the rest of the Canterbury coast but is mostly caused by Kaikoura's higher hazard from local and regional tsunamis (Power 2013b). Despite this scenario not representing as high a hazard level in the Kaikoura district it was still felt a worthwhile scenario to model to gain a feeling for how a bigger distant-source event than previously modelled would affect Kaikoura.

This report models a tsunami generated by such an earthquake and reports the resulting inundation in the following regions:

- Kaikoura and surrounds
    - Clarence River mouth
    - Hapuku to Kaikoura
    - South Bay and Peketa
    - Goose Bay and Oaro
- Pegasus Bay
    - Motunau
    - Waikuku Beach and Woodend Beach
    - The Pines/Kairaki/Kaiapoi
- Christchurch and Banks Peninsula
    - Christchurch

- Lyttelton Harbour coastal margin

- Akaroa Harbour coastal margin

- South Canterbury

    - Taumutu village and the margins of Lake Ellesmere

    - Rakaia River mouth (including north and south huts)

    - Rangitata River mouth (including north and south huts)

    - Browns Beach (Opihi River to Waipopo and up the Orari River mouth)

    - Seaforth to Scarborough (including Washdyke, Timaru, Saltwater Creek)

    - Pareora River mouth (including Pareora Village and freezing works)

See Figure 1-1 and Figure 1-2 for extents of the regions where inundation by tsunami were modelled. As a credible but conservative scenario, the base line water level for the modelling is set at Mean High Water Spring (MHWS). This represents the case where the largest wave arrives in conjunction with high tide for an average spring tide. If there is a train of large waves, at least one wave will probably arrive close to high tide. If there is a single wave considerably larger than all the other tsunami waves, then the state of the tide when that wave arrives is important. The difference between the maximum wave arriving in conjunction with high tide or with low tide can be up to 1.8 m in Kaikoura or up to 2.4 m in Lyttelton (which represent their tidal ranges (New Zealand Nautical Almanac (NZ204) 2012)) or more if non-linear interaction occurred. MHWS for Kaikoura for 2009-2010 is reported as 0.983 m above Lyttelton Vertical Datum 1937 (LVD37) in Goring (2010) and so in this modelling we have used the rounded value of 1 m above LVD37 for Kaikoura. For Pegasus Bay and further south we have used 1.2 metres above LVD37 as MHWS, which represents the height of MHWS-10 as measured at the Sumner sea level gauge (Bell 2011).
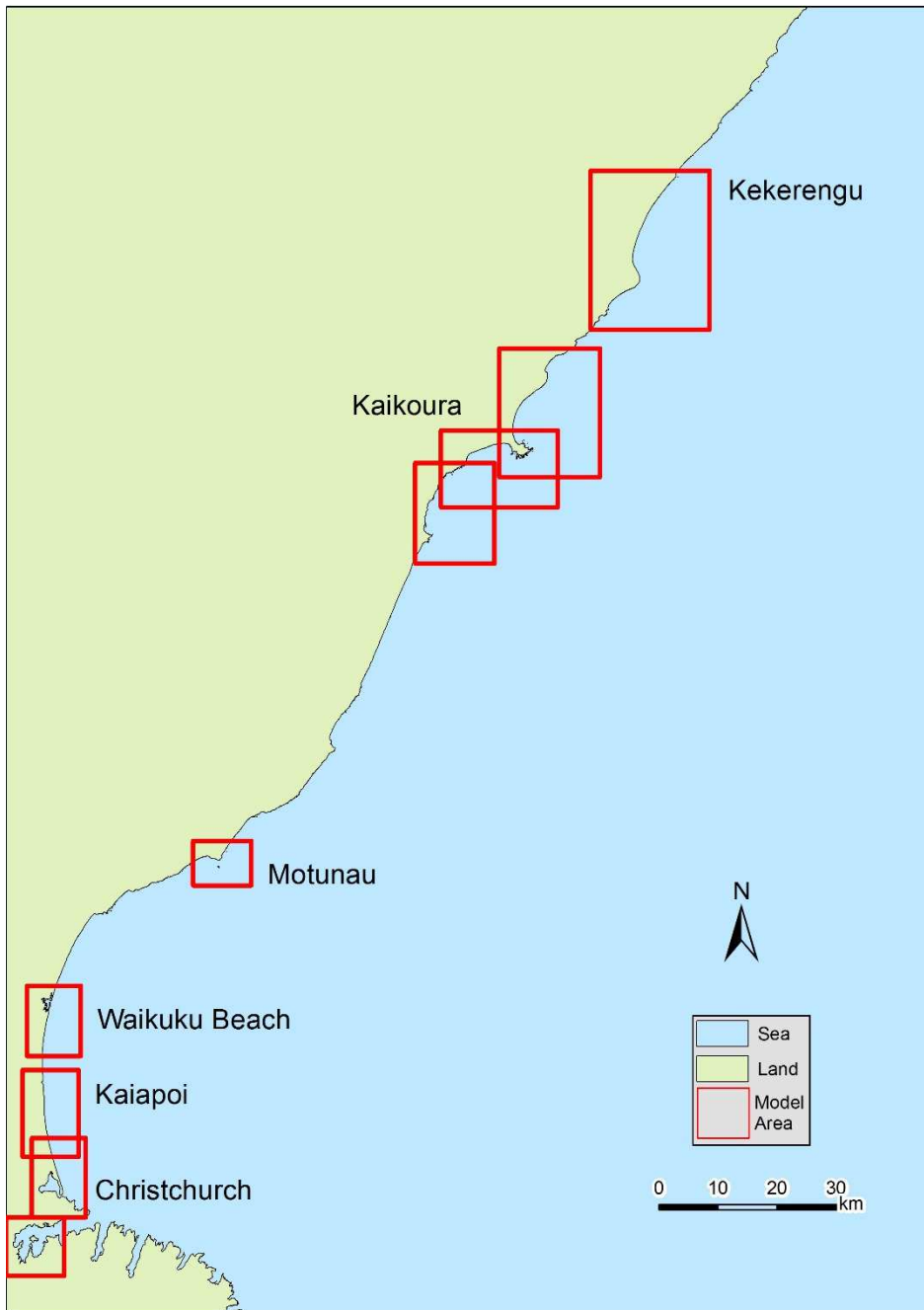
Figure 1-1: **Map of North Canterbury showing the locations of the areas where inundation was modelled**
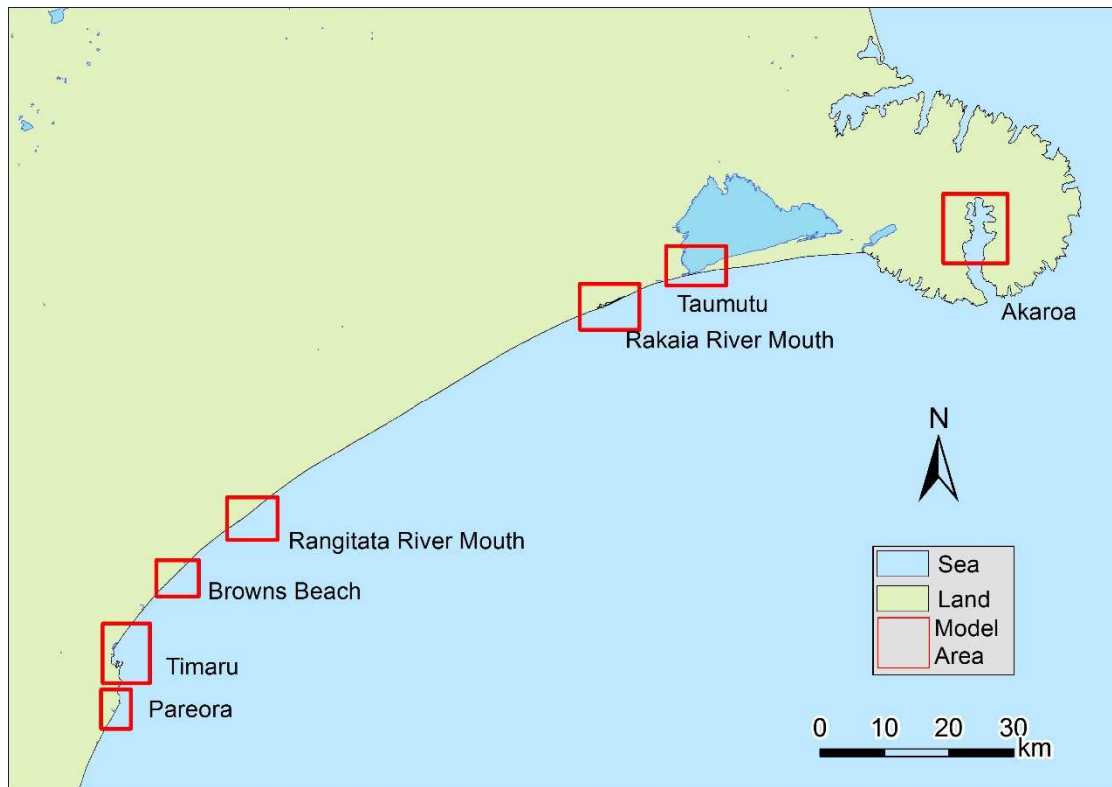
Figure 1-2:   Map of South Canterbury showing the locations of the areas where inundation was modelled.

2   The South American tsunami source

The source is specified off the coast of Peru. The deaggregation of the probabilistic tsunami modelling in the 2013 Tsunami Review (Power 2013a) identified Peru as a major source of tsunami hazard at the 2,500 year return period for almost all the Canterbury coast (It does not play as large a role in the risk to the Kaikoura coast (Kekerengu to Conway Flat) but this is due mainly to the existence of significant local and regional tsunami hazard rather than no hazard from South America). For a conservative inundation estimate the magnitude required to produce a wave height at coast equivalent to the 2,500 year 84th percentile level for Christchurch was chosen. This was similar in magnitude to sources required for similar tsunami hazard in other areas in Canterbury except Kaikoura.

Four possible sources with the same magnitude and similar epicentre were modelled. The initial water levels of these scenarios are shown in Figure 2-1 and their maximum wave heights across the Pacific are show in Figure 2-2. A moment magnitude of M_w 9.485 is equivalent to a seismic moment, M_0, of 2.1×10^{30} dyn cm. Shear Modulus, μ, for the earth's crust is generally taken to be between 2×10^{11} and 3.5×10^{11} dyn/cm^2 (1 dyne = 1^{-5} N). Using the relationship $M_0 = \mu A \bar{d}$ we thus assume an area (A) times average slip ($\bar{d}$) of 9×10^{12} m^3. Subduction zone interfaces tend to be $150 - 200$ km wide so for our scenarios we have an area of 150 km by 1,500 km with 40 m slip, an area of 200 km by 1,500 km with 30 m slip, and areas of 150 km by 2,400 km and 200 km by 1,800 km with 25 m of average slip. These scenarios are all located near the sites of the 1868 and 1877 Arica earthquakes.
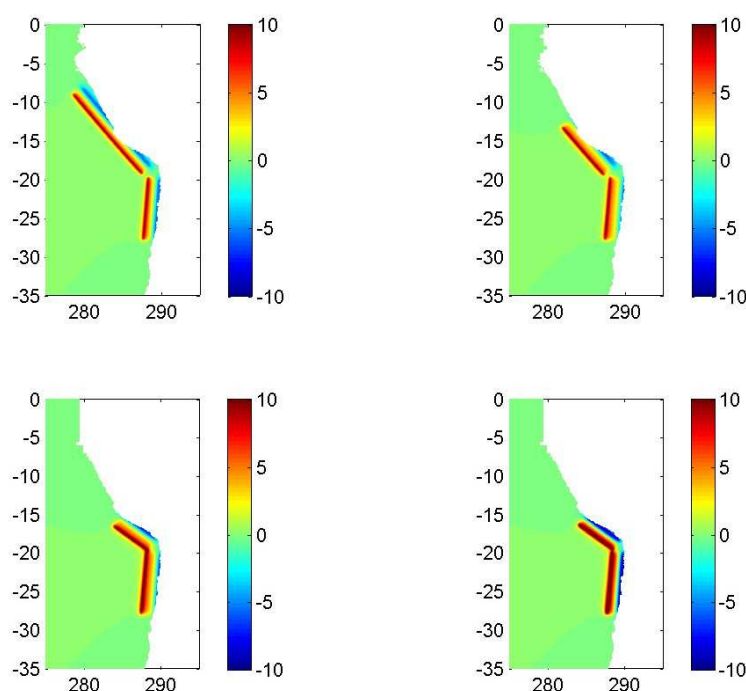
Figure 2-1:   Initial conditions for the four scenarios modelled. Top left: 25 m slip, 150 km by 2,400 km; top right: 25 m slip, 200 km by 1,800 km; bottom left: 30 m slip, 200 km by 1,500 km; bottom right: 40 m slip, 150 km by 1,500 km. The colour scale shows initial water level in metres.
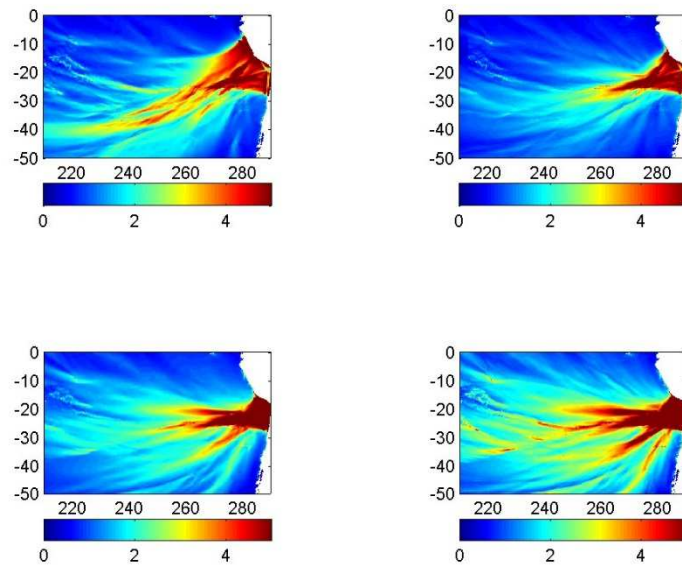
Figure 2-2: **Maximum wave height over the Pacific Ocean for four scenarios modelled.** Initial conditions are as shown in Figure 2-1. The colour scale shows maximum wave height in metres.

3   Modelling tsunami inundation

Modelling of tsunami waves were conducted in two phases. Firstly, far-field modelling was used to model the tsunami as it travels from its South American source across the Pacific Ocean. Then a near-field model was used to simulate the propagation of tsunami to the coast and on to land. The far-field model provides boundary conditions for the high resolution near-field and inundation modelling. These two models are described below.

3.1   Far-field modelling

The numerical model Gerris is used to model the tsunami from its source in the subduction zone off South America to the edge of the inundation grid. Gerris is a versatile numerical solver based on a quadtree adaptive mesh. As such it is able to adaptively refine and coarsen its grid to ensure that the model is well resolved where it needs to be to capture the tsunami waves. The Saint Venant Equations (also known as Non-linear Shallow Water Equations NSWE) were used to model the tsunami. For further details on Gerris and its tsunami modelling capabilities see Popinet (2003, 2011).

The tsunami waves were modelled across the Pacific Ocean and time series of the water height and velocities were output at the boundary points of the RiCOM grid. These were used as input into the RiCOM inundation model. Figure 2-1 and Figure 2-2 show the initial conditions and the overall maximum wave heights from the Gerris modelling.

3.2   Near-field and inundation modelling

3.2.1   Inundation models

The propagation of the tsunami from approximately 197° E to the coast and inundation of land was modelled using RiCOM (River and Coastal Ocean Model) developed by Roy Walters. This model had been developed over many years and has been used for tsunami inundation modeling for a range of scenarios (Walters and Casulli 1998a; Walters 2005a; Walters 2005b; Walters, Barnes et al. 2006a; Walters, Barnes et al. 2006b; Lane, Walters et al. 2007a; Lane, Walters et al. 2007b; Walters, Lane et al. 2007; Walters, Lane et al. 2009; Gillibrand, Power et al. 2010; Gillibrand, Arnold et al. 2011; Lane, Gillibrand et al. 2011).

RiCOM is based on the Reynolds-averaged Navier-Stokes (RANS) equations and the incompressibility criterion. For this modelling the hydrostatic assumption (that the vertical pressure gradient is balanced by gravity) is also made which reduces the equations to the non-linear shallow water equations (NLSWE). Research has shown that these equations adequately model tsunami inundation in the case of non-breaking waves (Pederson 2008). The time steps the model solves for are handled by a semi-implicit numerical scheme that avoids stability constraints on wave propagation. The advection scheme is semi-Lagrangian, which is robust, stable, and efficient (Staniforth and Coté 1991). Wetting and drying of intertidal or flooded areas occurs naturally with this formulation and is a consequence of the finite volume form of the continuity equation and method of calculating fluxes (flows) through the triangular element faces. Friction is enhanced for shallow water to account for the turbulent nature of tsunami flows but a spatially varying bed roughness is not used. At open (sea) boundaries, a radiation condition is enforced so that outgoing waves will not reflect back into the study area, but instead are allowed to realistically continue "through" this artificial boundary and into the open sea. The equations are solved with a conjugate-gradient iterative solver. The details of

the numerical approximations that lead to the required robustness and efficiency may be found in Walters and Casulli (1998b) and Walters (2005b).

The model is run with an initially quiescent sea state set at a level chosen to represent the tidal height at the arrival of the maximum wave (in this case MHWS). Timeseries of wave heights and velocity from the far-field (Gerris) modelling are applied at the boundary points of the inundation grids. Because of the difference in scales between tsunamis and sea waves, changes in the wave state do not significantly affect the tsunami inundation.

The simulation of inundation is strongly dependent on the quality of the topographic data and the bathymetric data in inshore waters. For this modelling we have LiDAR data for the land topography and high resolution LINZ hydrographic data for the near-shore bathymetry in the vicinity of Kaikoura and South Bay but in other areas the bathymetry is less well resolved.

Other uncertainties in the modelling study include the gridded representation of a continuous coastline, which can deform the shape of bays and estuaries, and the effects of building and land features on form drag. The latter could substantially modify the onshore propagation of tsunamis. Improving the drag representation remains a goal of current research. Eradication of the other errors is constrained by limitations of data quality and the practicalities of grid resolution; models always represent an approximation of reality.

Model uncertainty can be quantified by running multiple simulations with small variations in key parameters, an approach known as ensemble prediction or sensitivity analysis. Such an approach provides an envelope of predicted solutions, rather than single "worst-case" or "scenario-type" predictions, on which to base emergency response procedures. However, running many simulations increases the computational and research costs, and, in any event, model forecasts can never be certain because our knowledge of all the geophysical processes involved in tsunami generation, propagation and inundation remains incomplete. In this work here we run four scenarios with the same moment magnitude to cover a range of possible fault geometries.

Quantitative calibration of the tsunami inundation model against real measurements is difficult due to the uncertain nature of tsunami impact data from New Zealand and the consequent difficulty in identifying events from the past. Nevertheless, the RiCOM model has been continuously validated against standard analytical test cases (e.g. Walters and Casulli 1998b; Walters 2005b; Walters 2005a), and model predictions of run-up height for this scenario have compared well to palaeotsunami data in the Bay of Plenty (Walters, Goff et al. 2006) and along the Otago coastline (Goff, James R., Lane et al. 2009).

3.2.2   Inundation model grid – bathymetry and topography

RiCOM uses an irregular, unstructured grid built up of triangles. As such, it is able to smoothly grade between different resolutions without requiring nested models. The triangles must be close to equilateral to minimise numerical error (Henry and Walters 1993). The grid was created using a combination of GridGen (Henry and Walters 1993) and TriQGrid (NIWA in-house software).

A bathymetric grid covering New Zealand's Exclusive Economic Zone (EEZ) was used as a base grid. This was cut down to cover from the east coast of New Zealand (East Cape to Dunedin) to 197° E. In the open ocean it has a resolution around 2 km which is refined to around 500 m at the coast. In the areas of interest in this study it is further refined to 10-20 m and a land grid at a similar resolution is created and attached to the bathymetric grid to create a seamless inundation grid. The land grid

covers the areas of interest expected to be inundated. Inundation grids have been developed with specific high resolution where it is needed for inundation including stopbanks resolved around the Waimakariri and Avon rivers and a sea wall in Sumner. Figure 3-1 shows an example of the full grid used for the tsunami modelling and Figure 3-2 shows a close-up of the land grid for Christchurch and Kaiapoi. Eight grids were used in total which were developed during the previous tsunami modelling reports (Gillibrand, Arnold et al. 2011; Lane, Arnold et al. 2012; Lane and Arnold 2013). Open ocean bathymetry at 30 second resolution (GEBCO 2013) was incorporated with NIWA in-house bathymetry for coastal New Zealand. LiDAR data provided by Environment Canterbury was used to create the land topography. The vertical datum used in the grid is Lyttelton Vertical Datum 1937 (LVD37).
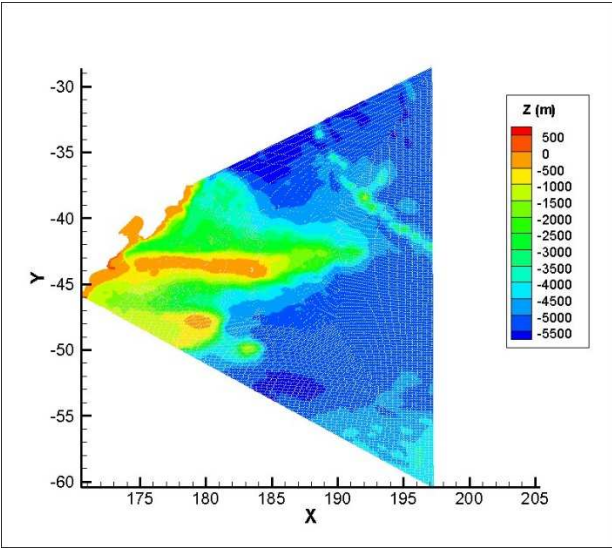
Figure 3-1: **The full grid used for tsunami modelling.** Colour represents water depth
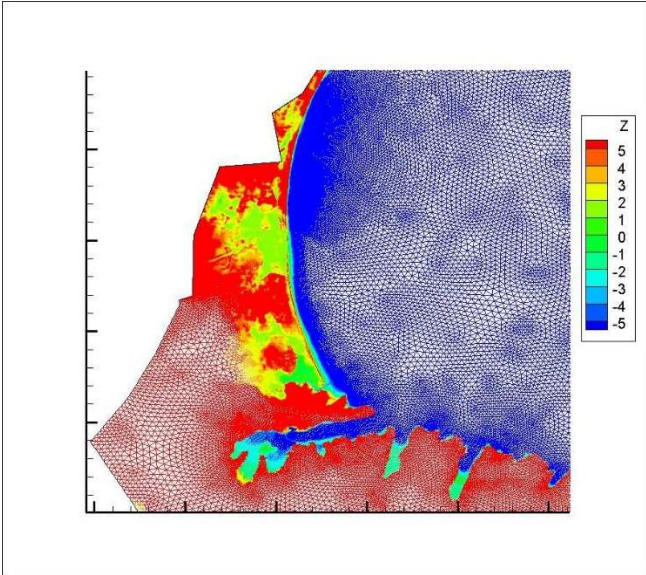
Figure 3-2: **Close up of Christchurch and Kaiapoi inundation grid.** The grid is coloured by depth between -5 metres and 5 metres to emphasise the coastal regions. The size of the elements grades in towards the coastline, evidenced by the solidifying of the colouring which represents very fine resolution. Resolution of the land grid of interest is generally 10-15 m. Resolution is finer around the Waimakariri and Avon stop bank in order to resolve these features.

3.3   Model outputs

The numerical model was used to provide the following outputs which describe the propagation and magnitude of the tsunami arriving at the Canterbury coastline, and the inundation at the specified locations:

A.   Maps of maximum wave heights (relative to mean sea level). These are taken as the maximum of the four scenarios modelled, so maximum wave heights in different areas may represent different scenarios, although the overall pattern was similar in all cases.

B.   Spatial data depicting the depth and extent of coastal inundation at the specified areas for the largest wave arriving at MHWS. These are taken as the maximum of the four scenarios modelled, so inundation depths in different areas may represent different scenarios, although the overall pattern was similar in all cases. The inundation depth is the depth of water on land (i.e. it is not referenced to mean sea level). If this data is used with a topographic representation different from that used in the model spurious results may occur.

C.   Spatial data depicting the maximum flow speed over land in the specified areas for the largest wave arriving at MHWS. These are taken as the maximum of the four scenarios modelled, so maximum speeds in different areas may represent different scenarios, although the overall pattern was similar in all cases.

In this report, the spatial maps are presented and discussed. The spatial data (in ArcGIS format) is provided to Environment Canterbury along with this report in the CD enclosed as Appendix A.

For information about potential risk to humans due to water depth and velocity see Figure 2.1 in (H R Wallingford, 2006) or Table 5 in (Cox et al. 2010). Also it should be noted that the maximum inundation depth and maximum water speed shown in this report do not necessarily occur simultaneously and so could conservatively overestimate the hazard.

4   Model results

The first tsunami wave generally arrives at the Canterbury coast between 14 to 15 hours after the fault rupture. There was some variation between the different scenarios but all four showed similar general patterns. The largest wave tends to arrive later around 17-20 hours after fault rupture. Often there is a chain of large waves which can last until at least 24 hours after fault rupture. Generally after then the wave energy gradually decreases but there can still be large disturbances until at least 24 hours after the arrival of the first wave (i.e. around 40 hours after fault rupture). Because there wasn't one scenario that was larger than all the others the following results present the maximum values over the four scenarios.

4.1   Maximum wave height

The maximum predicted tsunami elevation for the northern part of the Canterbury coast is shown in Figure 4-1 and for the southern part of the Canterbury coast is shown in Figure 4-2. The values in this figure are given relative to the undisturbed water level and do not include the MHWS offset the inundation modelling includes. The actual water level can be obtained by adding the tidal water level at the time of the wave arrival. These are the maximum of the four different scenarios. Water elevations due to the tsunami along the Canterbury coast are typically between 4 to 10 metres above the initial water level. The larger values (up to and over 10 m) are in Pegasus Bay and the bays on the north side of Banks Peninsula due to resonance effects. Note that the inundation modelling assumes a background sea level of 1 m in the Kaikoura region and 1.2 m in the rest of Canterbury to represent the height of MHWS above LVD37. Thus the tsunami elevation is at least 5 m above LVD37 (and over 11 metres above LVD37 in some areas) assuming the highest wave coincided with MHWS.

4.2   Maximum inundation and speed

Maps of maximum inundation depth and maximum flow speed are presented for each study location. Maximum inundation is the inundation that would occur if the arrival of the largest wave at a particular location (not necessarily the first wave and not necessarily the same wave in different areas) coincided with MHWS. In this simulation the second wave is usually the largest in this region. Maximum inundation and speed maps here are for illustration purposes only. The full GIS digital spatial data files are included on CD as Appendix A. Figure 1-1 shows the extents that the tsunami inundation modelling maps cover. For each location a figure showing maximum inundation depth and another showing maximum flow speed are given. Inundation depths are only given over the land, whereas speeds are given for the sea as well as inundated areas of the land. Results are given from north to south. The GIS files should be consulted for further details. Note that the maximum inundations and water speeds may not necessarily occur during the same wave or the same scenario.
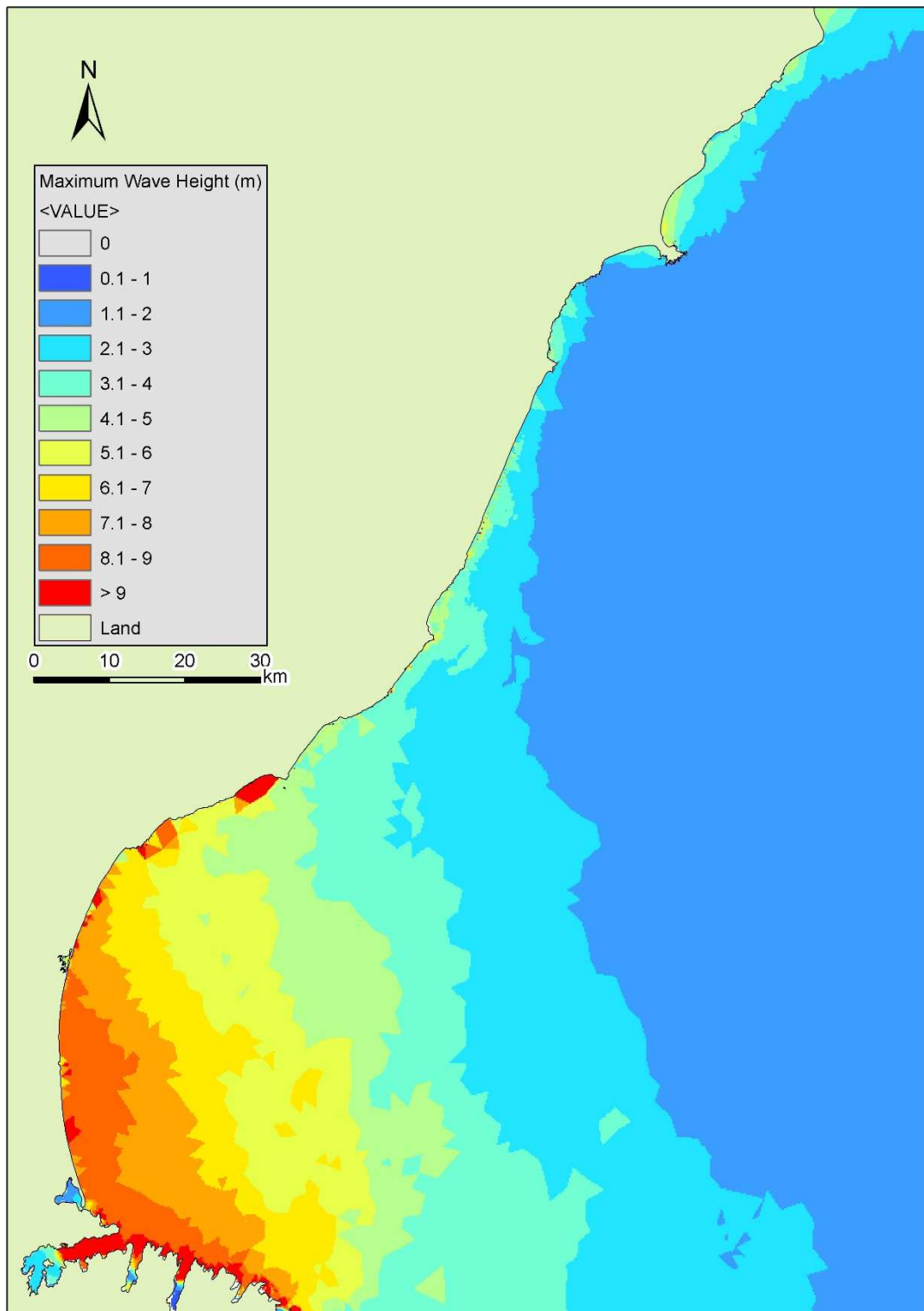
Figure 4-1: **Predicted maximum water elevations (m) along the North Canterbury coastline.** The actual maximum water level reached during the tsunami event can be calculated by adding the value from this figure to the tidal level at the arrival of the largest wave.

Figure 4-2:   Predicted maximum water elevations (m) along the South Canterbury coastline. The actual maximum water level reached during the tsunami event can be calculated by adding the value from this figure to the tidal level at the arrival of the largest wave.
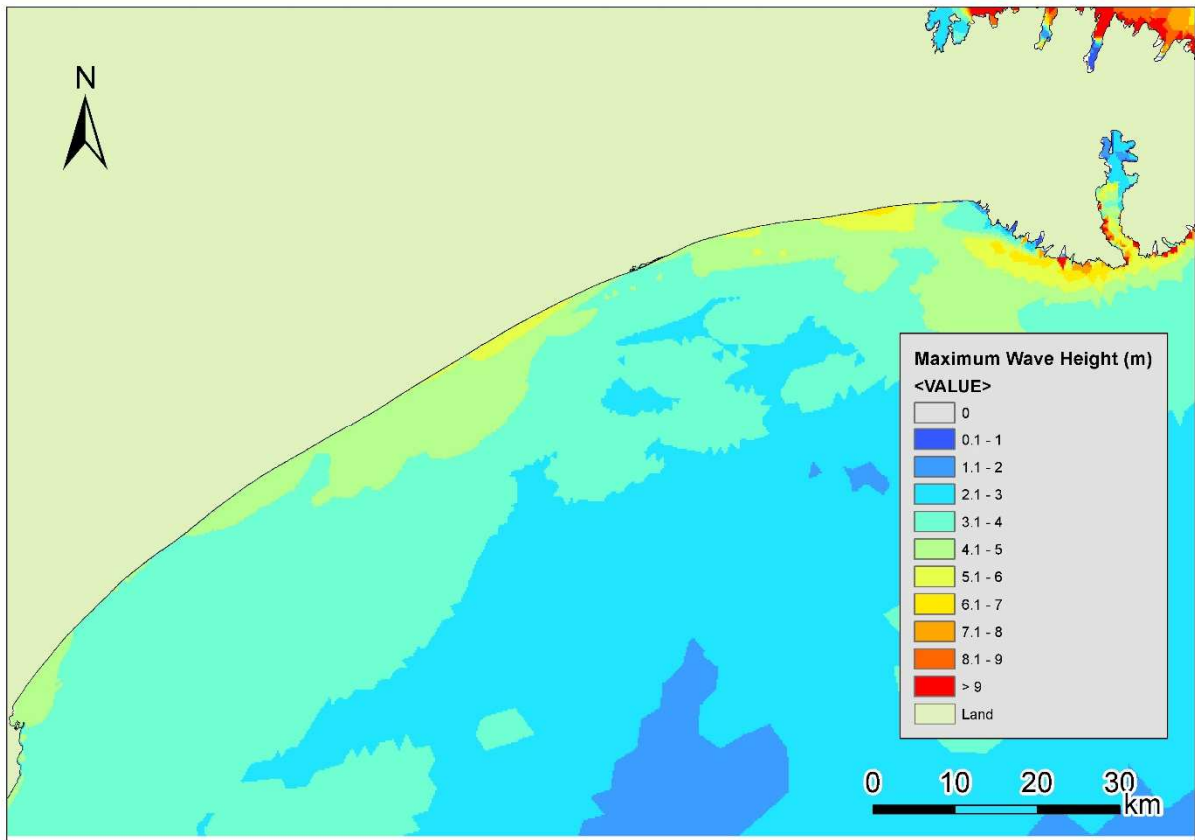
4.2.1   Kekerengu to Clarence River Mouth

Maximum inundation depths are shown for the region from Kekerengu to the Clarence River Mouth in Figure 4-3 and maximum speed is shown in Figure 4-4. Inundation extends close to State Highway 1 along much of the strip between Kekerengu and the Clarence River Mouth and may reach the road in places. Depths are over 2.5 metres deep and maximum speeds are over 3 m/s in places near the shoreline. Water in the Clarence River (not taken into account in our modelling) could allow surges to travel further up-river than shown in this modelling.
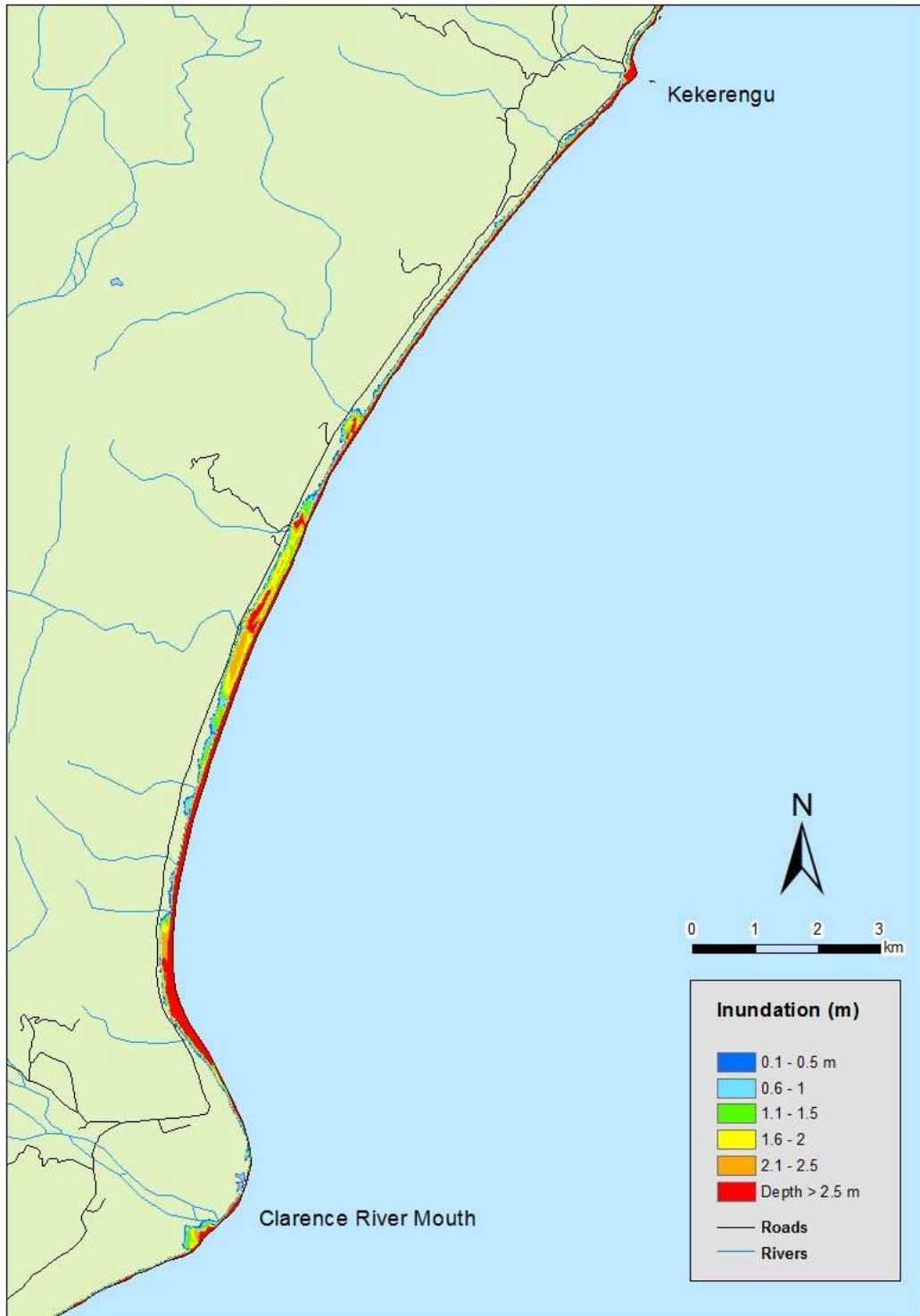
Figure 4-3:   Maximum inundation depth for Kekerengu to Clarence River Mouth assuming the largest wave arrived at MHWS. Inundation depths are only shown for inundated land.
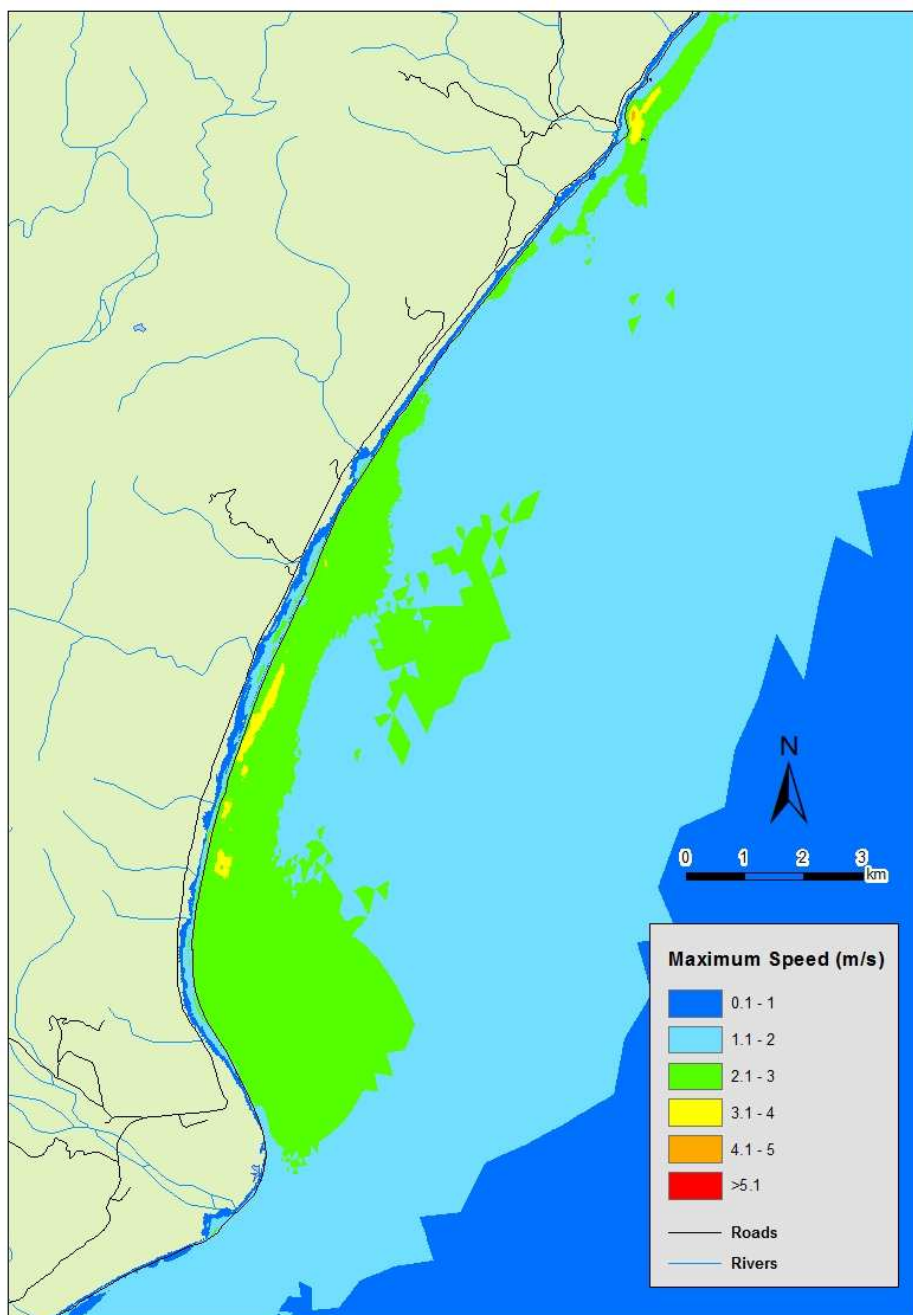
Figure 4-4: **Maximum flow speed for Kekerengu to Clarence River Mouth assuming the largest wave arrived at MHWS.**

4.2.2 Hapuku to Kaikoura

Maximum inundation for the region from Hapuku to Kaikoura is shown in Figure 4-5 and maximum speed is shown in Figure 4-6. Inundation reaches close to State Highway 1 at Mangamaunu and near the coast road just south. Water in the Hapuku River (not taken into account in our modelling) could allow surges to travel further up-river than shown in this modelling. On the north side of Kaikoura Peninsula there is inundation of Esplanade, Lower Ward St, Avoca St, Fyffe Quay and the lower ends of Killarney St, Yarmouth St, Brighton St, Ramsgate St, Margate St and Torquay St. On the south side of Kaikoura Peninsula there is inundation of South Bay Parade, Moa St, Tui St, Kaka St and Weka St. This inundation is over 2 m in places. Most of the low lying coastal strip on the Peninsula is inundated. Water speeds reach up to 3 m/s in places.
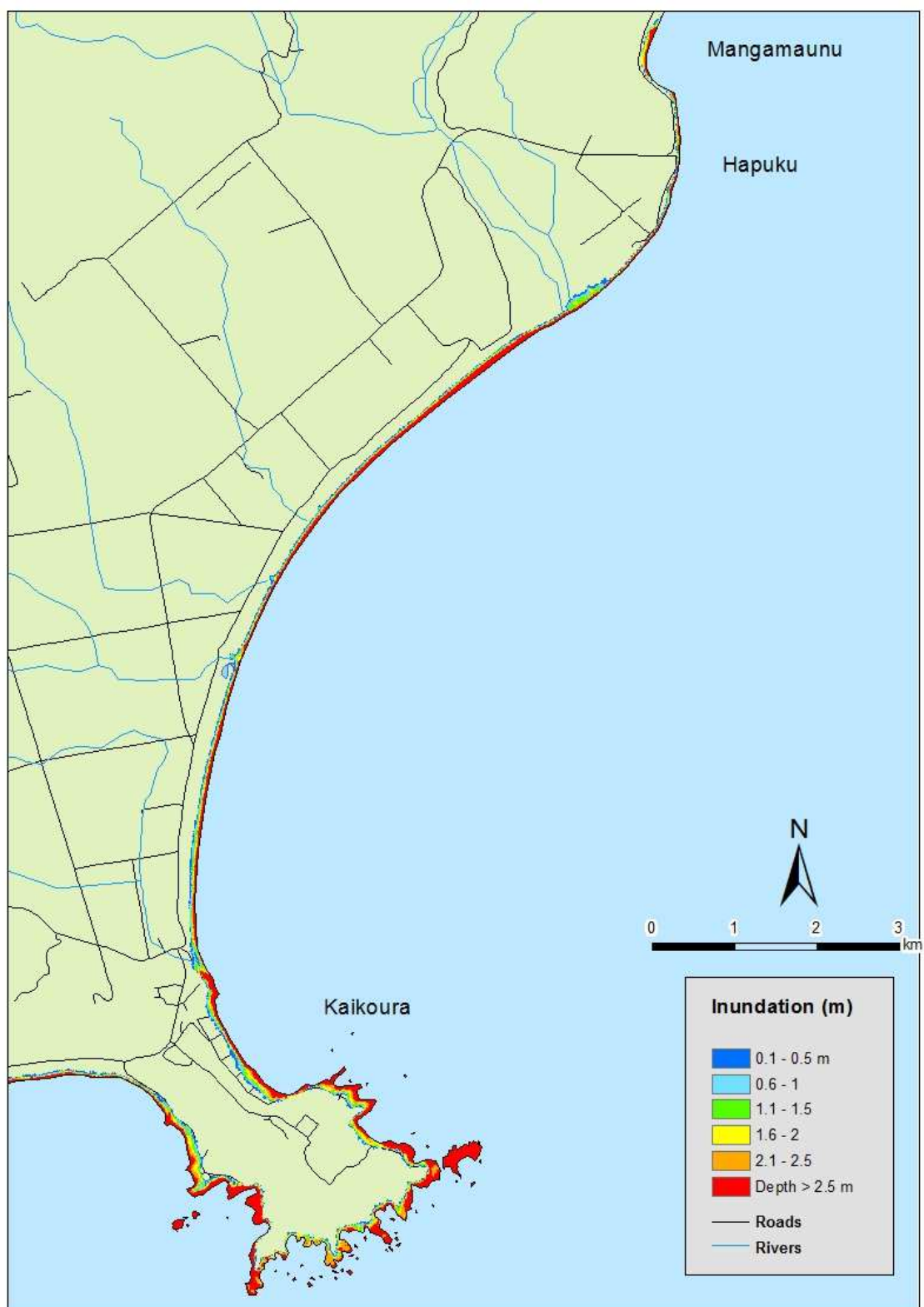
Figure 4-5: **Maximum inundation depth for Hapuku to Kaikoura assuming the largest wave arrived at MHWS.** Inundation depths are only shown for inundated land.
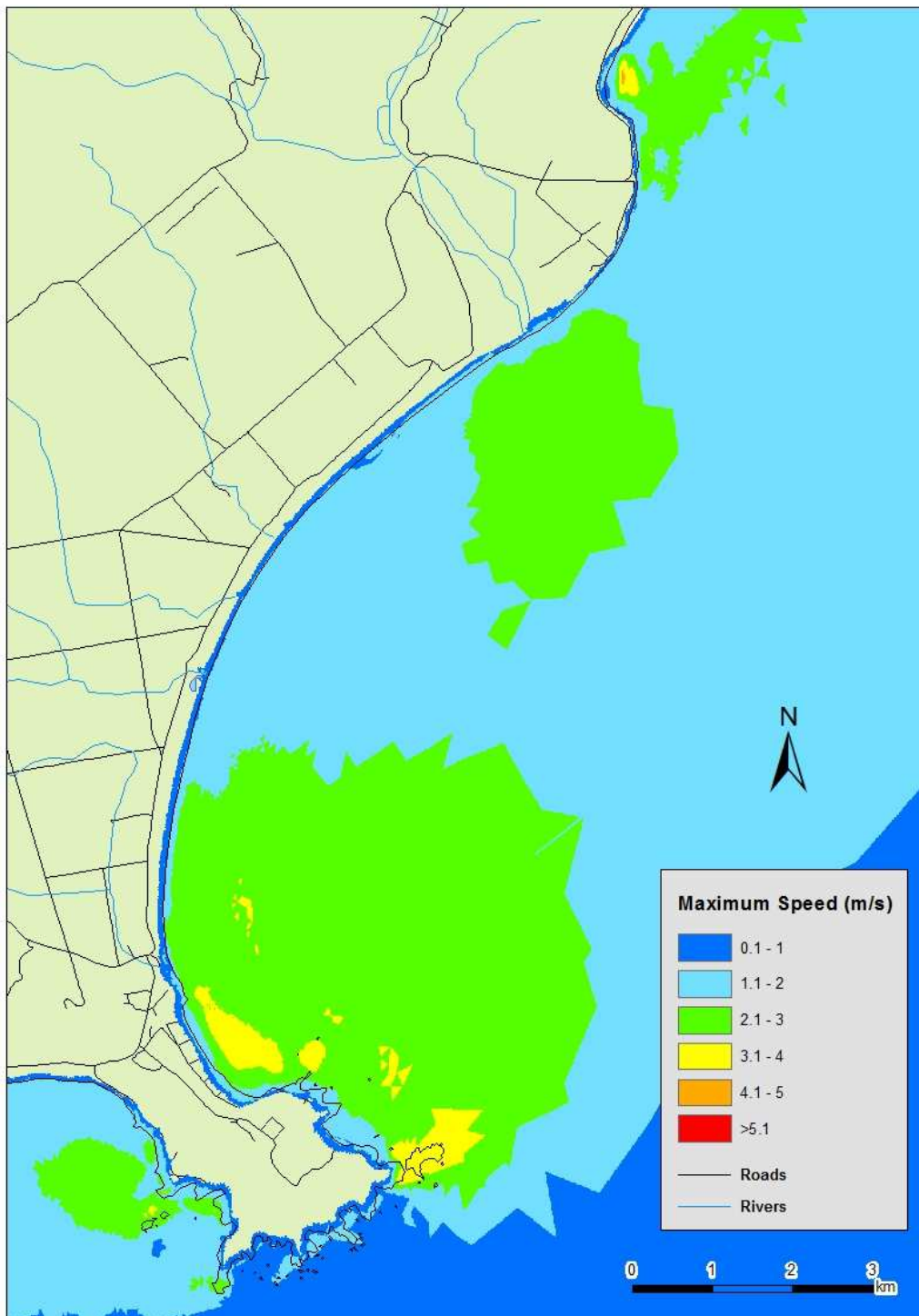
Figure 4-6: **Maximum flow speed for Hapuku to Kaikoura assuming the largest wave arrived at MHWS.**

4.2.3   South Bay and Peketa

Maximum inundation depths and speed for South Bay and Peketa are shown in Figure 4-7 and Figure 4-8 respectively. Most of South Bay is inundated in up to 2 m water. Inundation just reaches State Highway 1 on the south end of Peketa and possibly also along the coastal strip. Flow speeds are higher on the north side of the Peninsula but can reach up to 3 m/s just offshore of South Bay.

Figure 4-7: **Maximum inundation depth for South Bay and Peketa assuming the largest wave arrived at MHWS.** Inundation depths are only shown for inundated land.

Figure 4-8: **Maximum flow speed for South Bay and Peketa assuming the largest wave arrived at MHWS.**

4.2.4   Goose Bay and Oaro

Maximum inundation and maximum speed for the area including Goose Bay and Oaro are shown in
Figure 4-9 and Figure 4-10 respectively. The wave reaches the State Highway several places between
Goose Bay and Oaro and inundates a large part of Oaro. Flow speeds reach up to 4 m/s offshore of
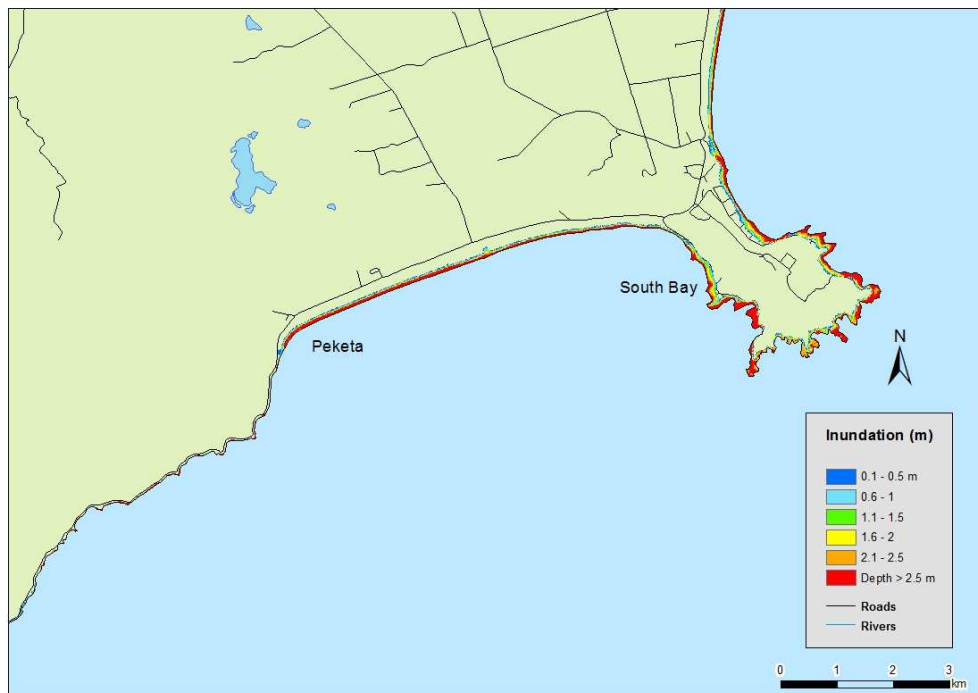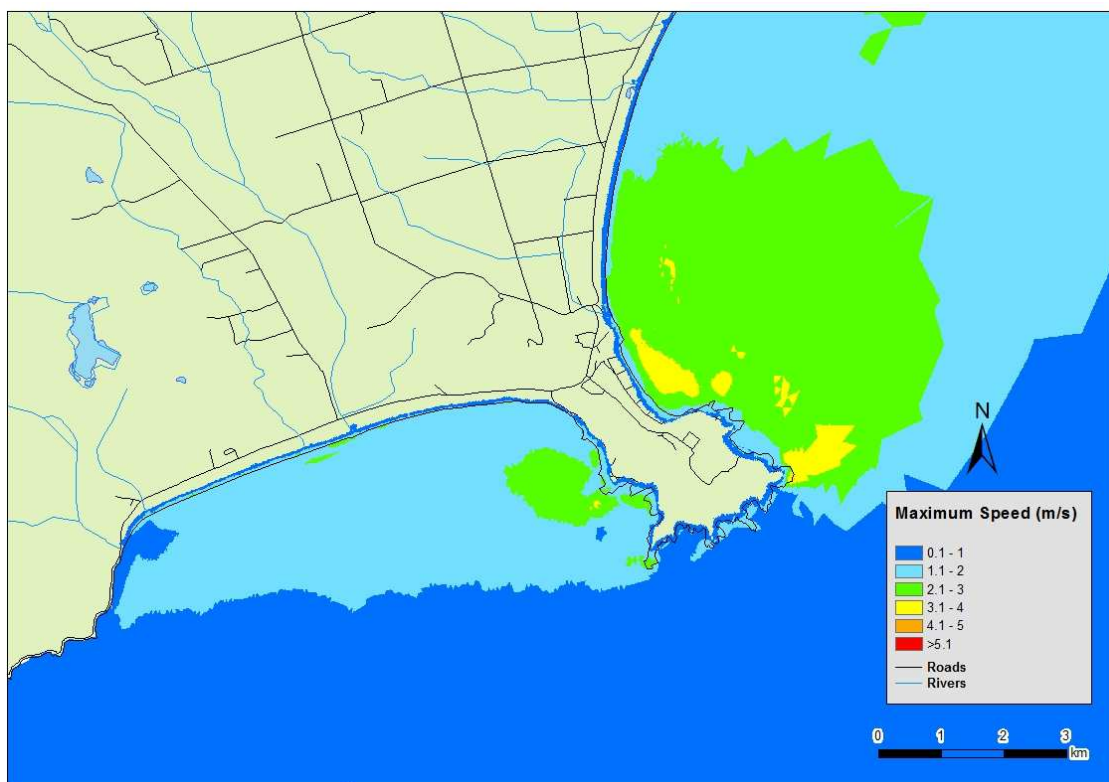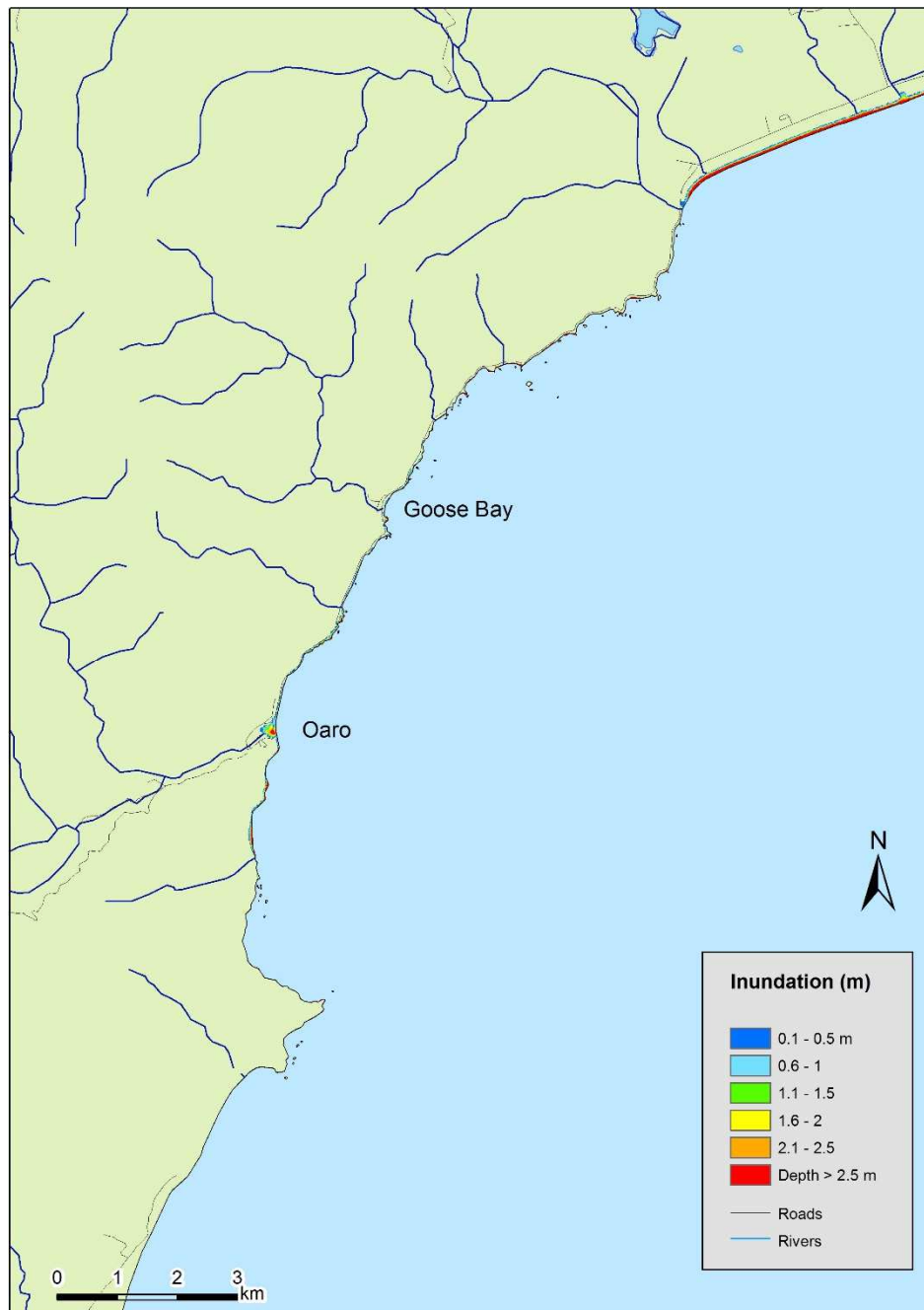Oaro.

**Figure 4-9:   Maximum inundation depth for Goose Bay and Oaro assuming the largest wave arrived at
MHWS.** Inundation depths are only shown for inundated land.

Figure 4-10: Maximum flow speed for Goose Bay and Oaro assuming the largest wave arrived at MHWS.

4.2.5   Motunau

Maximum inundation and maximum flow speeds for Motunau are shown in Figure 4-11 and Figure 4-12 respectively. The tsunami travels up the river and inundates The Parade in Motunau. The beach to the south of Motunau is inundated to over 2.5 m. Flow speeds are up to 5 m/s offshore from Motunau. Water in the Motunau River (not taken into account in our modelling) could allow surges to travel further up-river than shown in this modelling.

Figure 4-11:   Maximum inundation depth for Motunau assuming the largest wave arrived at MHWS.
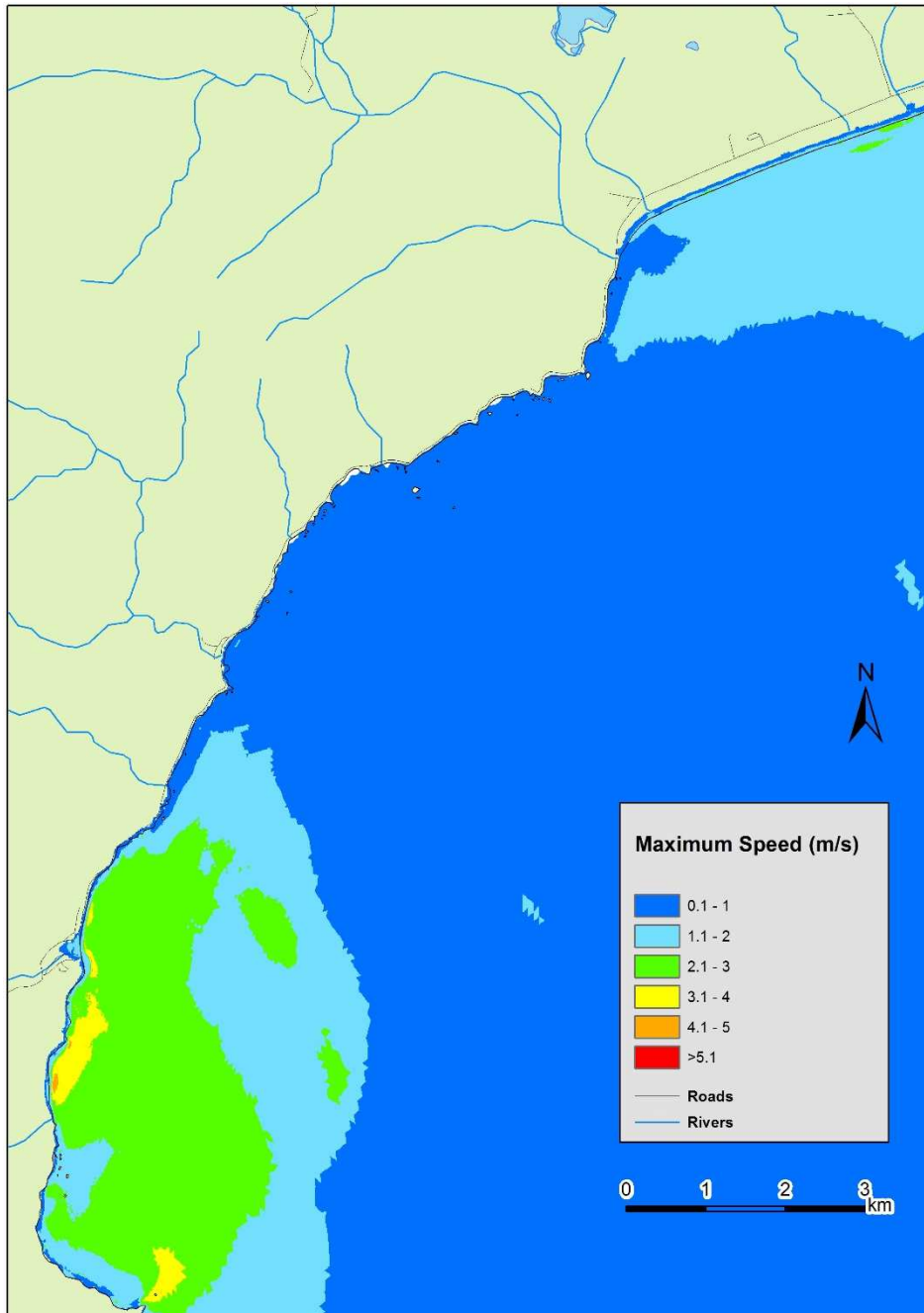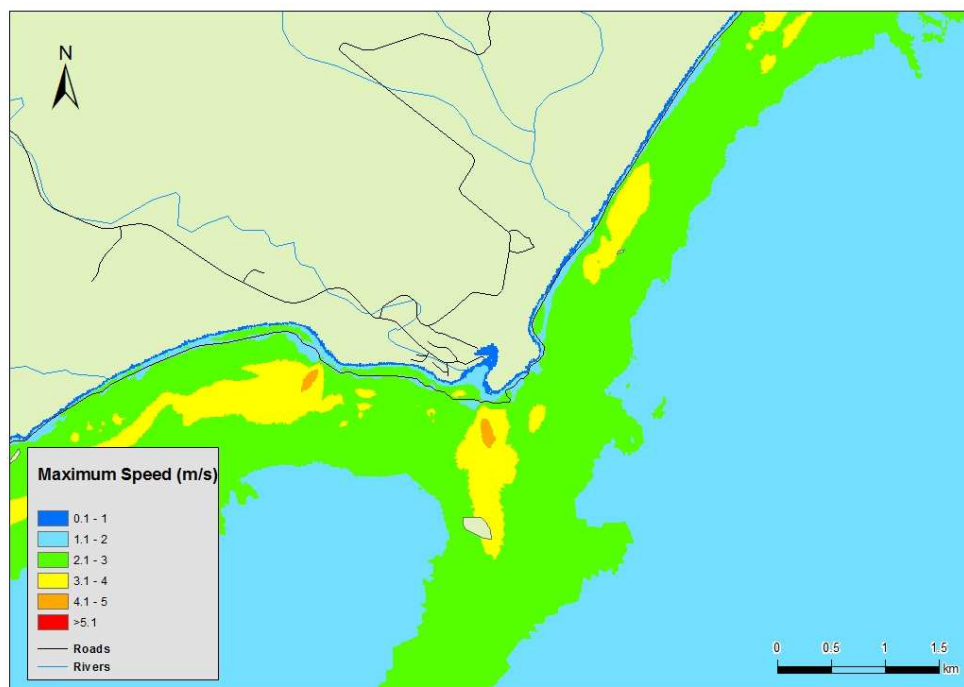Inundation depths are only shown for inundated land.

Figure 4-12:   Maximum flow speed for Motunau assuming the largest wave arrived at MHWS.

4.2.6 Waikuku Beach and Woodend Beach

Maximum inundation and maximum flow speed assuming the largest wave arrives at MHWS are shown in Figure 4-13 and Figure 4-14 respectively. Waikuku Beach is extensively inundated over 2 m deep in places. The Saltwater Creek area is also inundated although not as deeply. Flow speeds are up to 4-5 m/s in places. Water in the Ashley River (not taken into account in our modelling) could allow surges to travel further up-river than shown in this modelling.
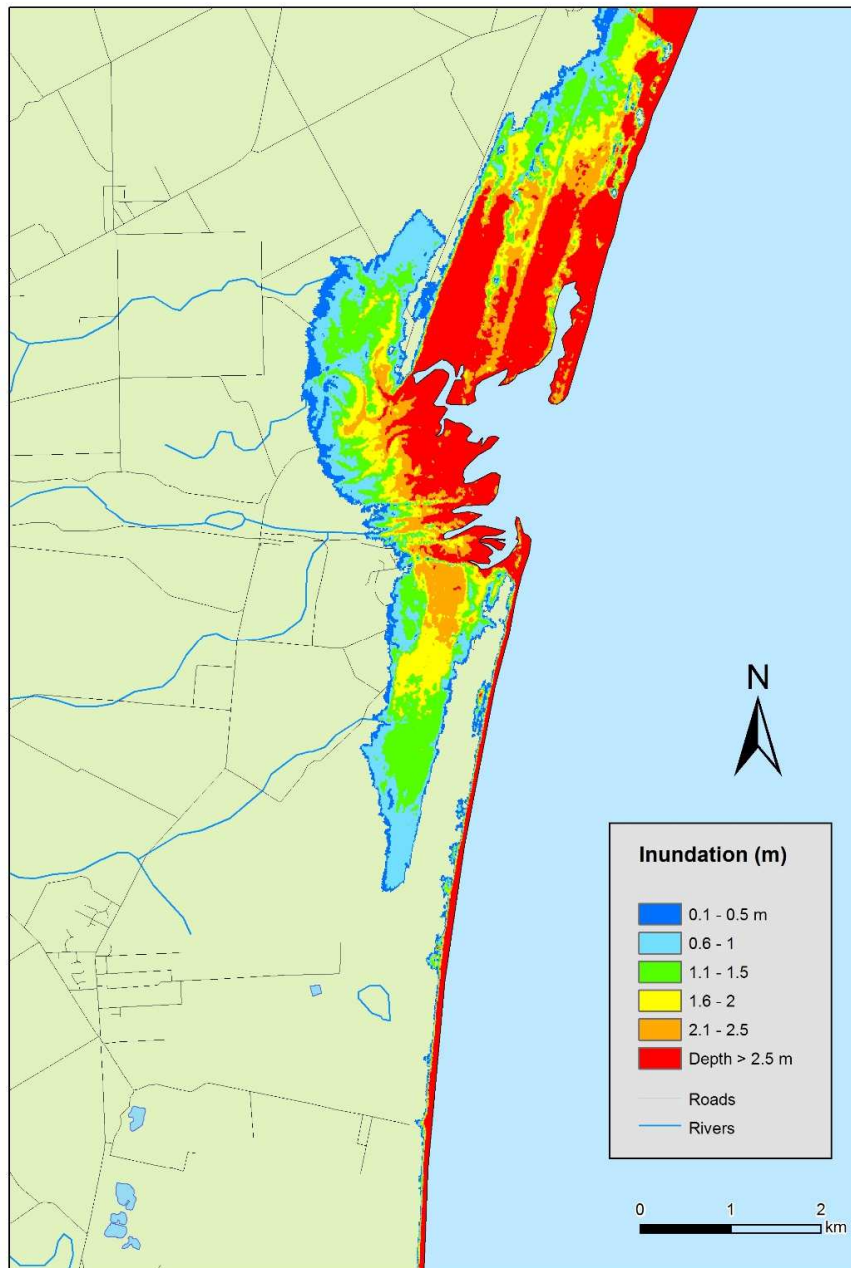

Figure 4-13: Maximum inundation depth for Waikuku Beach and Woodend Beach assuming the largest wave arrived at MHWS. Inundation depths are only shown for inundated land.
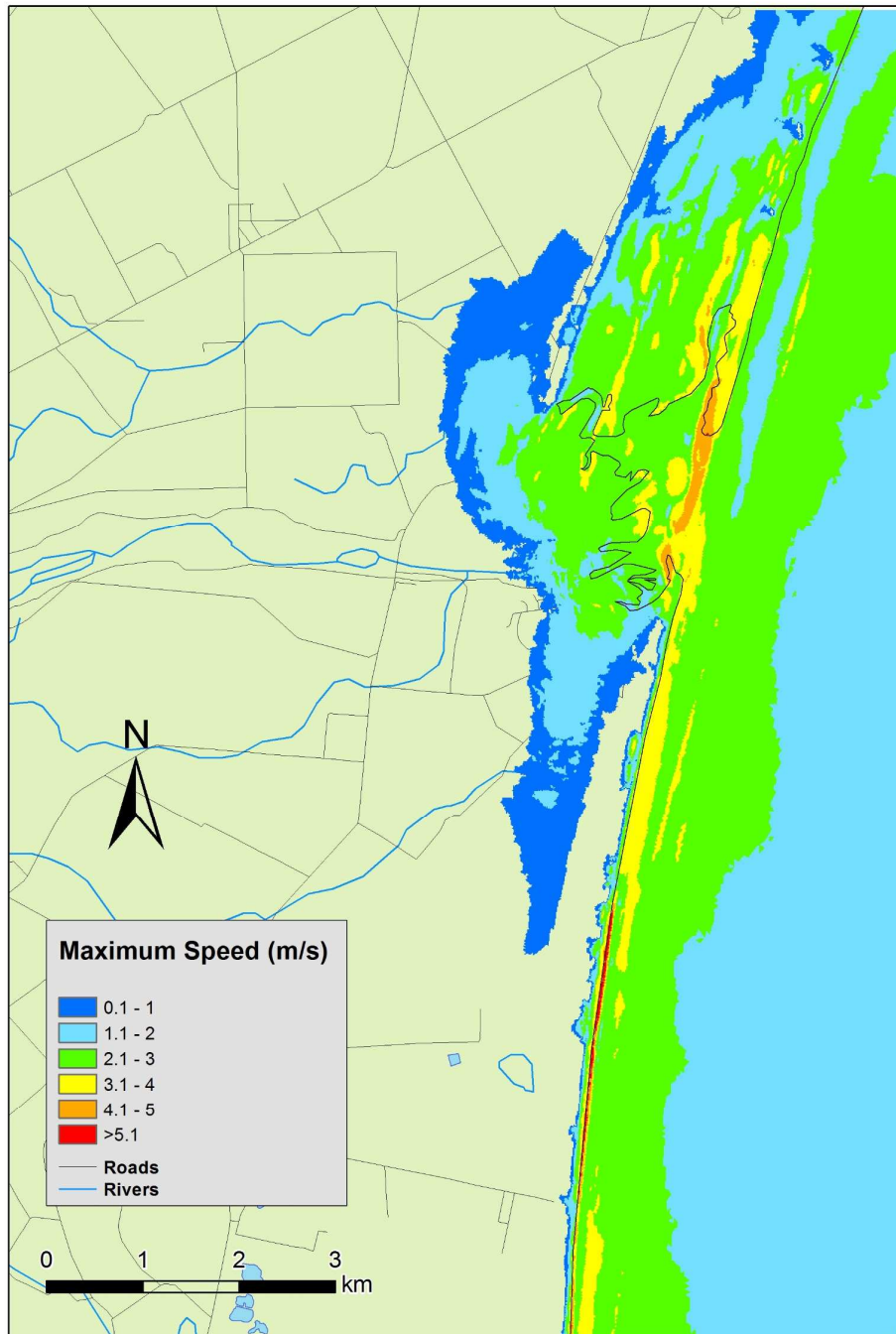
Figure 4-14:   Maximum flow speed for Waikuku Beach and Woodend Beach assuming the largest wave arrived at MHWS.

4.2.7 The Pines to Spencerville (including Kairaki, Kaiapoi, Brooklands)
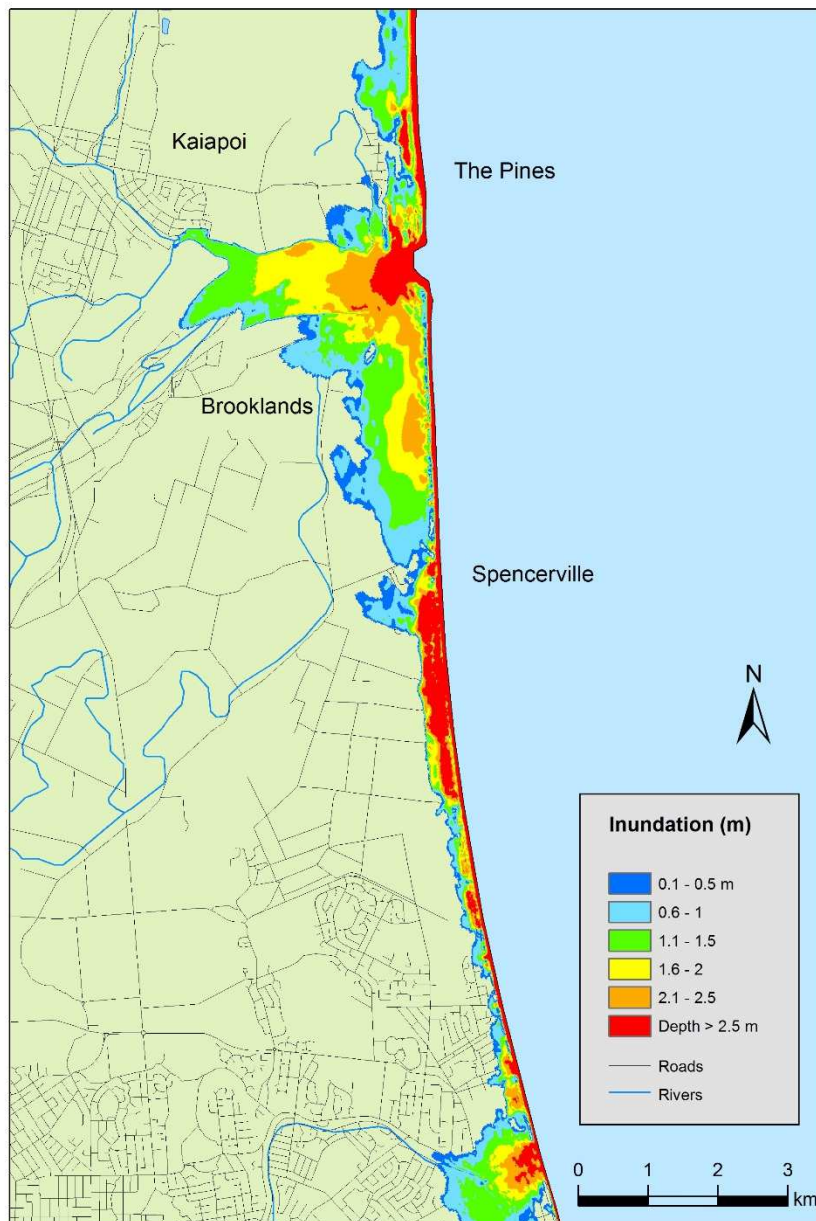
Figure 4-15:   Maximum inundation depth for The Pines, Kairaki, Kaiapoi, Brooklands and Spencerville assuming the largest wave arrived at MHWS.   Inundation depths are only shown for inundated land.

Maximum inundation and maximum speed assuming the largest wave arrives at MHWS for The Pines, Kairaki, Kaiapoi Brooklands and Spencerville are shown in Figure 4-15 and Figure 4-16 respectively. Kairaki is inundated under 1-2 m of water and this inundation reaches the edges of the Pines too. The stop banks seem to protect Kaiapoi and the oxidation ponds from the tsunami. Brooklands and Spencerville are also severely inundated. Water in the Waimakariri River (not taken into account in our modelling) could allow surges to travel further up-river than shown in this modelling.
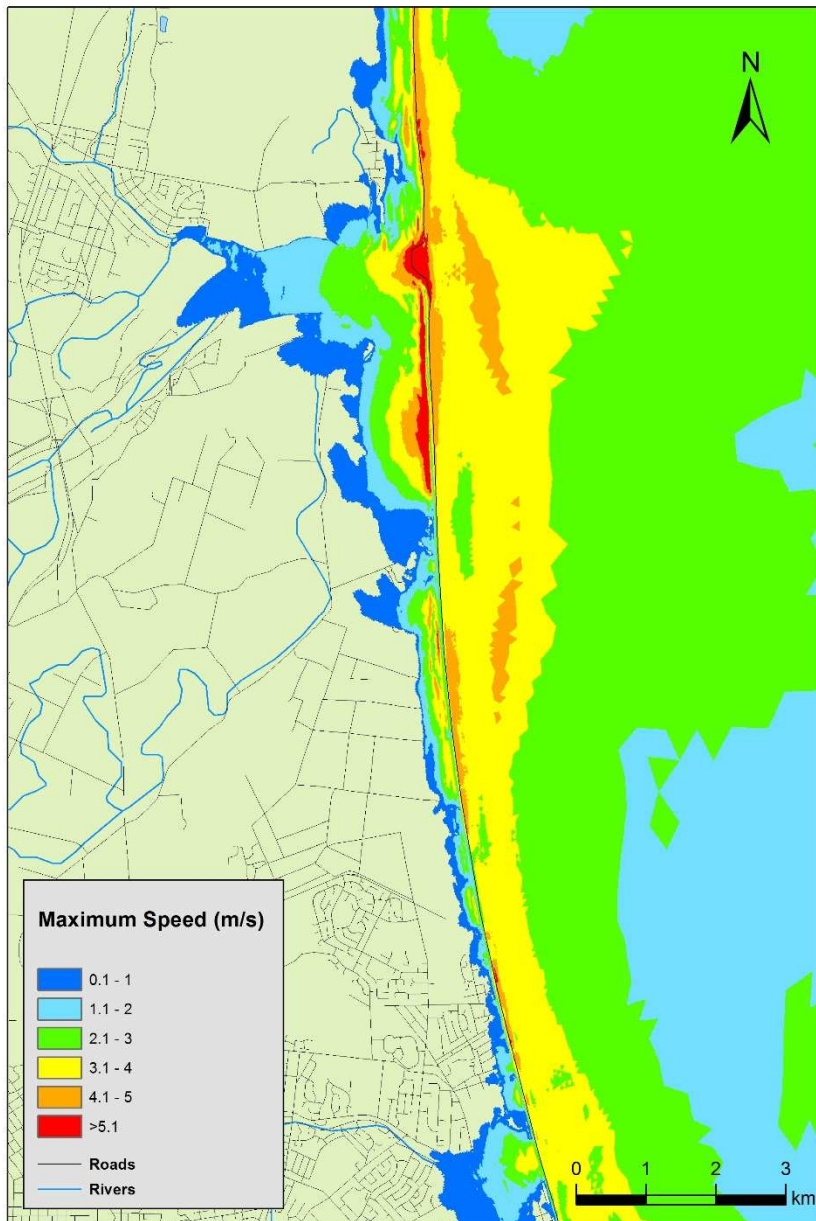
Figure 4-16:   **Maximum flow speed for The Pines, Kairaki and Kaiapoi assuming the largest wave arrived at MHWS.**

4.2.8   Christchurch

Figure 4-17 and Figure 4-18 show the maximum inundation depth and maximum speed for Christchurch assuming that the wave arrives at MHWS. Most of New Brighton, South Shore, Redcliffs, Sumner and Taylor's Mistake are inundated to over 2.5 m in many places. Bexley, the shoreward part of North New Brighton, Ferrymead and McCormack's Bay are also severely inundated. Flow speeds are over 5 m/s around the mouth of Ihutai-Avon-Heathcote Estuary.
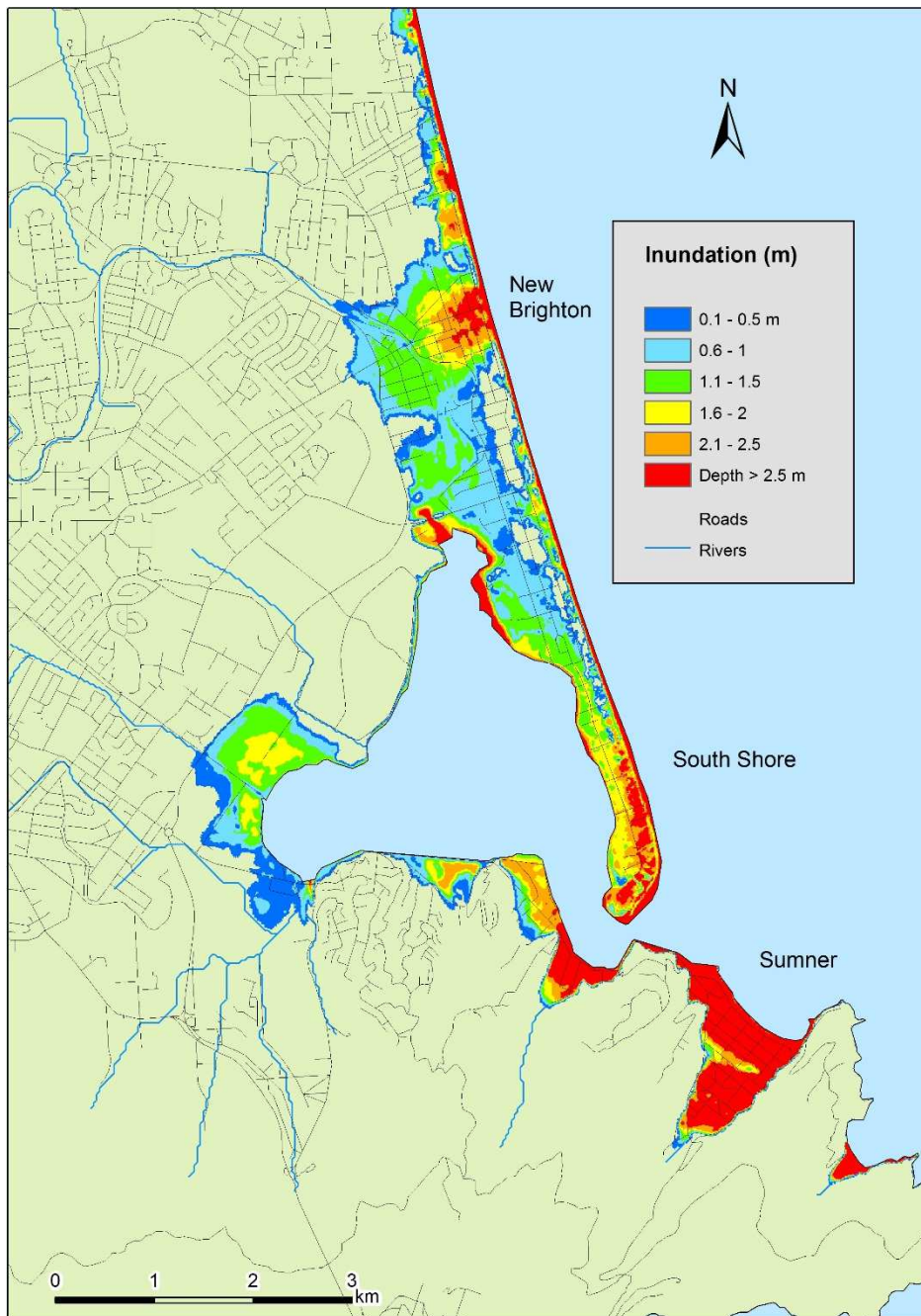
Figure 4-17:   Maximum inundation depth for Christchurch assuming the largest wave arrived at MHWS.
Inundation depths are only shown for inundated land.
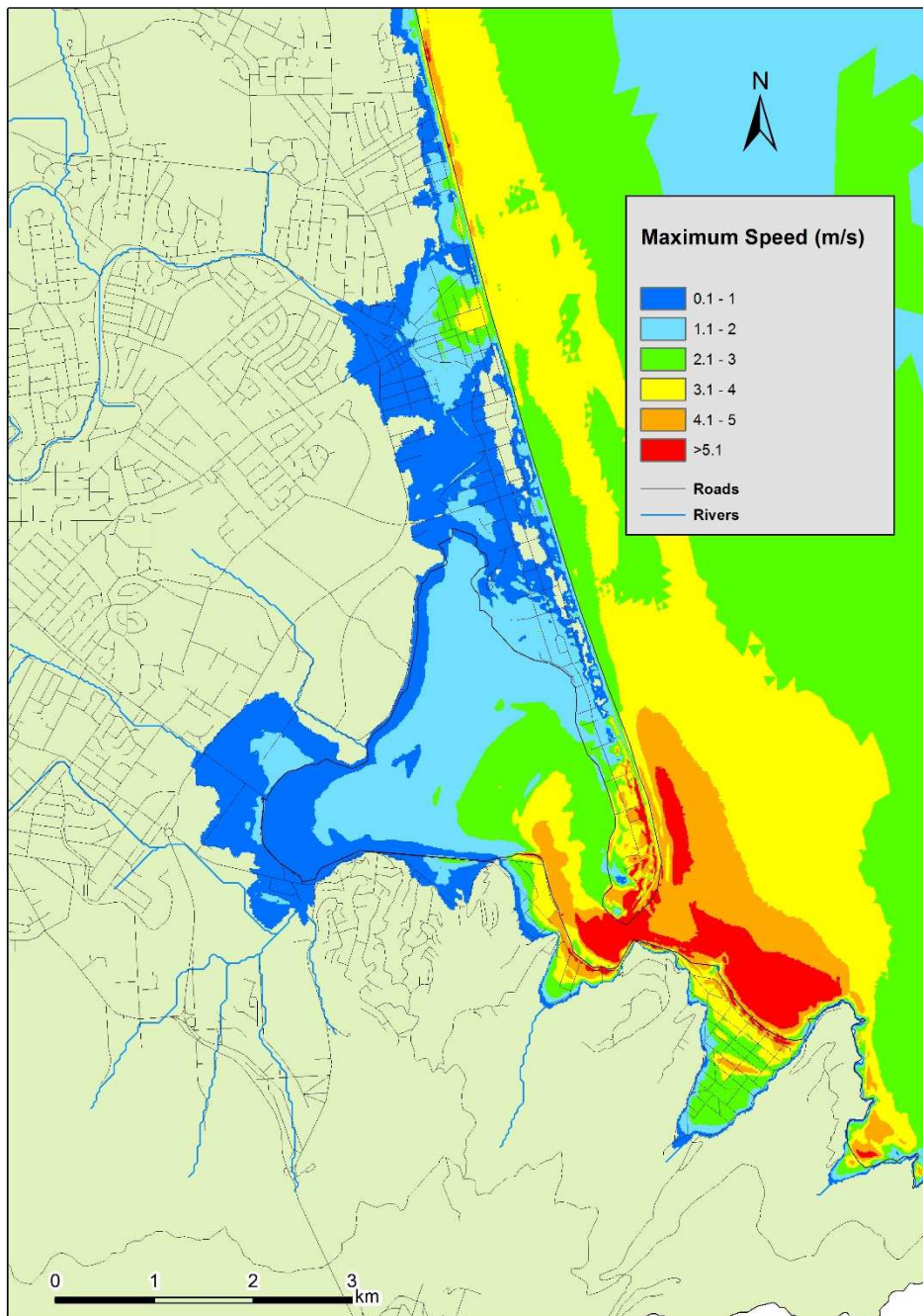
Figure 4-18: Maximum flow speed for Christchurch assuming the largest wave arrived at MHWS. Flow speeds are over 5 m/s in many areas near the estuary mouth.

4.2.9   Lyttelton Harbour

Figure 4-19 and Figure 4-20 show the maximum inundation depth and speed respectively for Lyttelton Harbour assuming that the largest wave comes in at MHWS. All the low lying port area of Lyttelton is inundated as are extensive low lying areas in Allandale, Teddington and Charteris Bay. There is also inundation along the coastal strip throughout the harbour. Flow speeds are up to 5 m/s especially around the opening to Lyttelton Port.
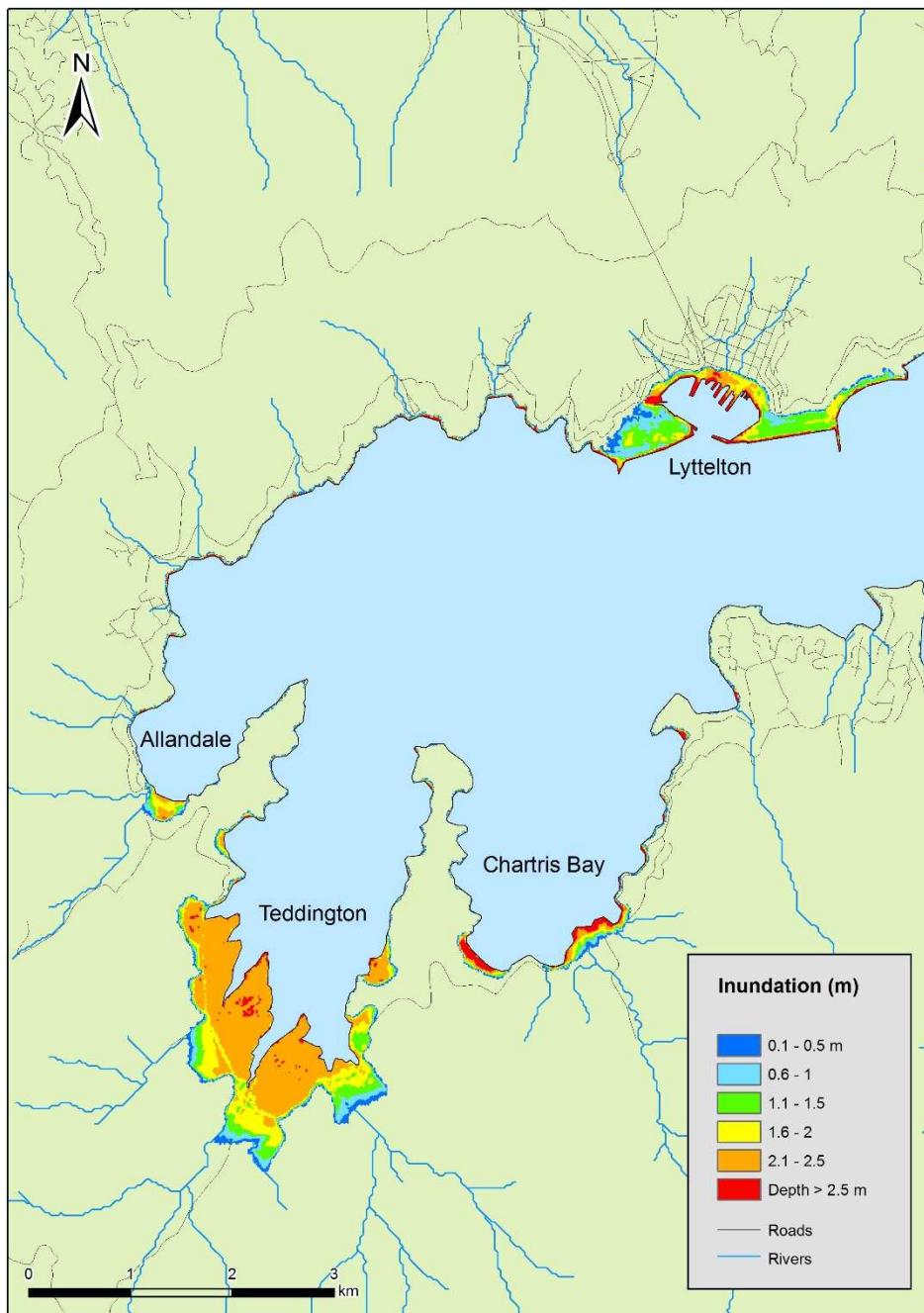
Figure 4-19: Maximum inundation depth for Lyttelton Harbour coastal margin assuming the largest wave arrived at MHWS. Inundation depths are only shown for inundated land.

Figure 4-20:   Maximum flow speed for Lyttelton Harbour coastal margin assuming the largest wave arrived at MHWS.

4.2.10 Akaroa Harbour

Figure 4-21 and Figure 4-22 show the maximum inundation and maximum flow speed respectively for Akaroa Harbour assuming that the largest wave arrives at MHWS. All the low lying part of Akaroa is inundated including the main street. The main road is also inundated at Barrys Bay, Duvauchelle Bay and Robinsons Bay. There is also inundation of low lying areas in Takamatua Bay, French Farm Bay and Wainui. Most of the coastal strip is also inundated. Flow speeds are up to 3 m/s in the harbour.

Figure 4-21: Maximum inundation depth for Akaroa Harbour coastal margin assuming the largest wave arrived at MHWS.   Inundation depths are only shown for inundated land.
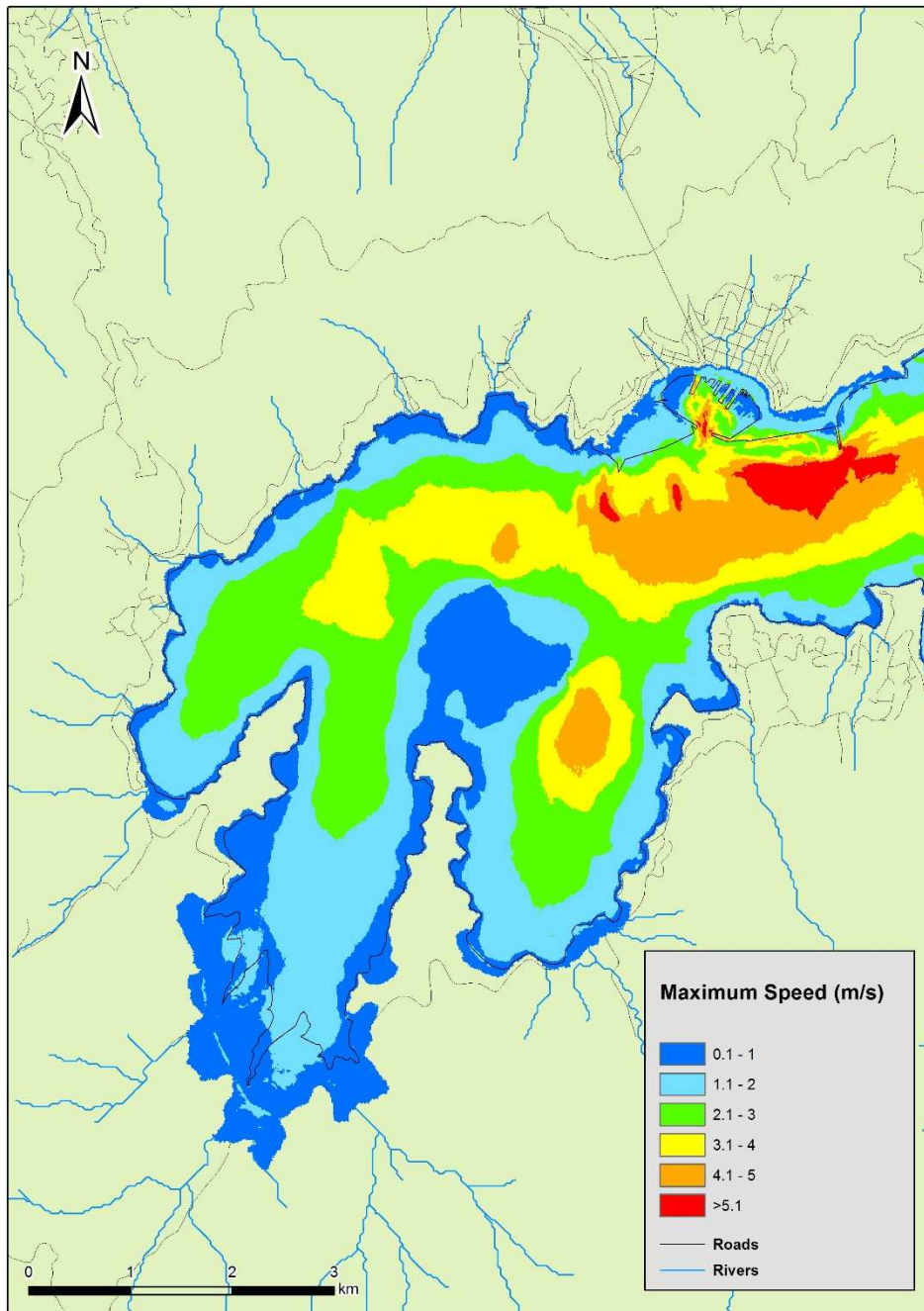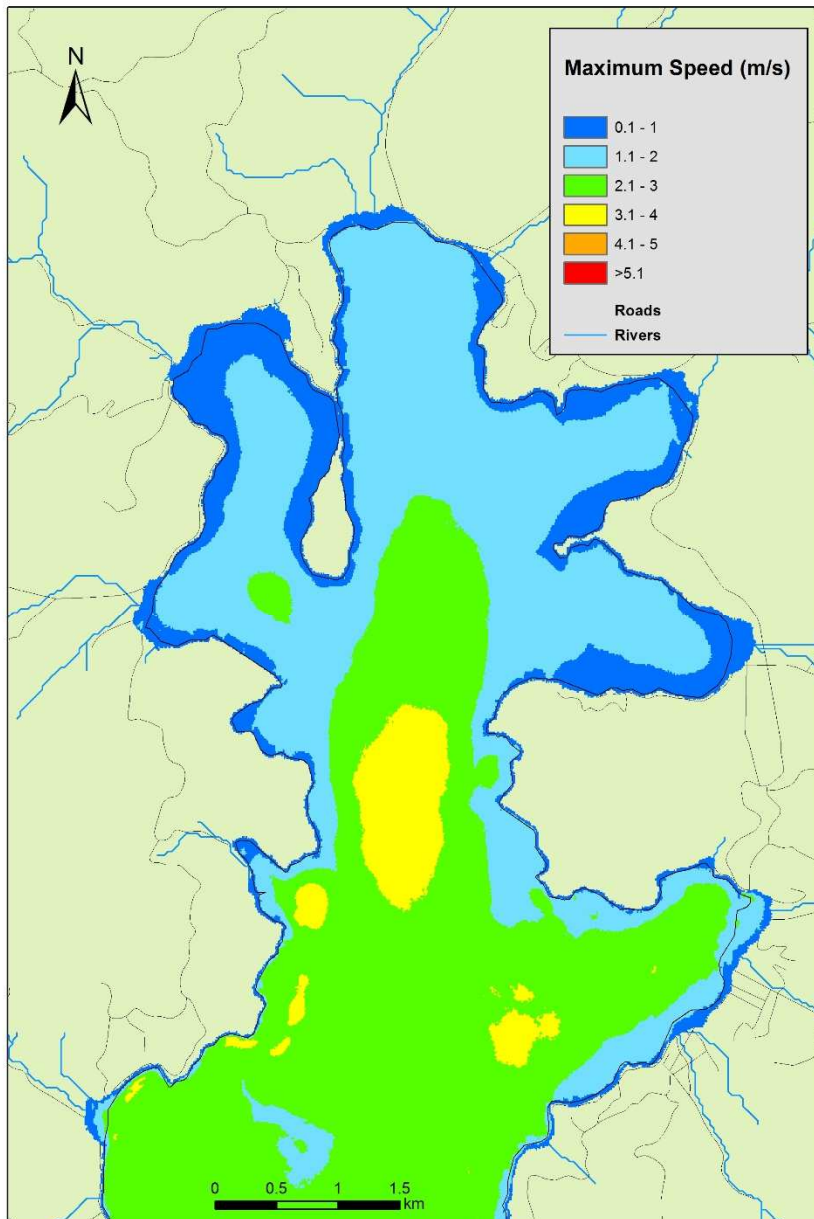
Figure 4-22: **Maximum flow speed for Akaroa Habour coastal margin assuming the largest wave arrived at MHWS.**

4.2.11 Taumutu village and the margins of Lake Ellesmere

Figure 4-23 and Figure 4-24 show the maximum inundation depth and maximum flow speed for Taumutu and the margin of Lake Ellesmere. This is modelled with the lake opening closed. The tsunami overtops Kaitorete Spit at the opening. Realistically this would probably cause a breach in the spit although this is not modelled here. That would allow later waves far more access into Lake Ellesmere. Flow speeds are less than to the north of Banks Peninsula reaching over 2 m/s.
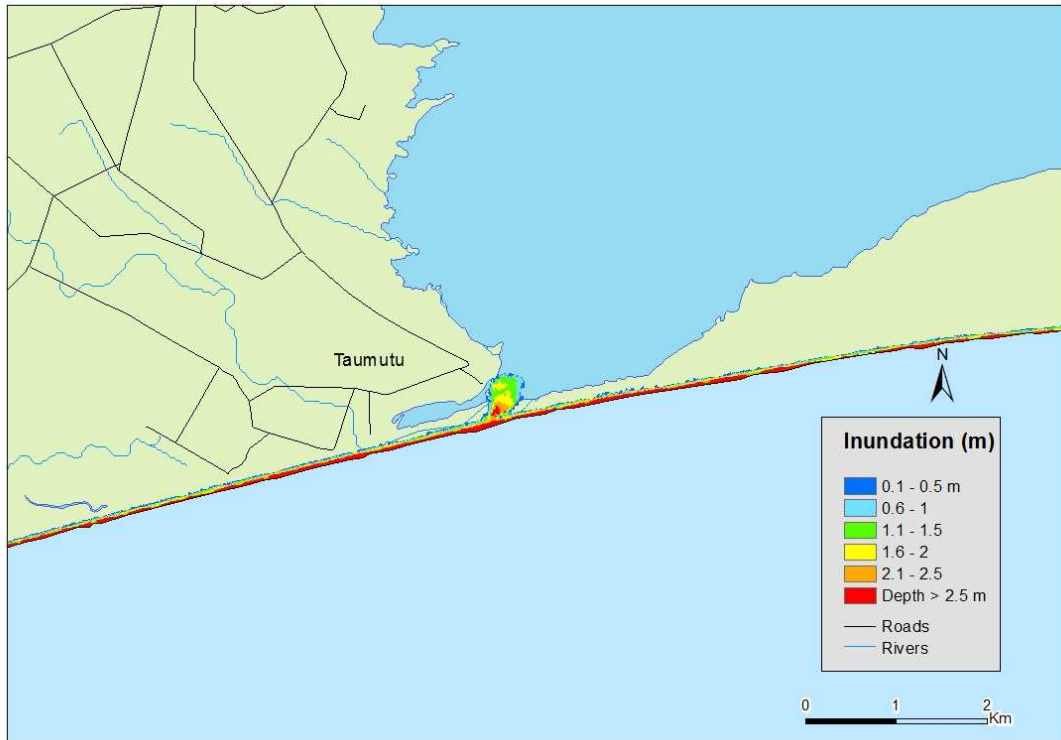
Figure 4-23: **Maximum inundation depth for Taumutu village and the margins of Lake Ellesmere assuming the largest wave arrived at MHWS.** Inundation depths are only shown for inundated land.
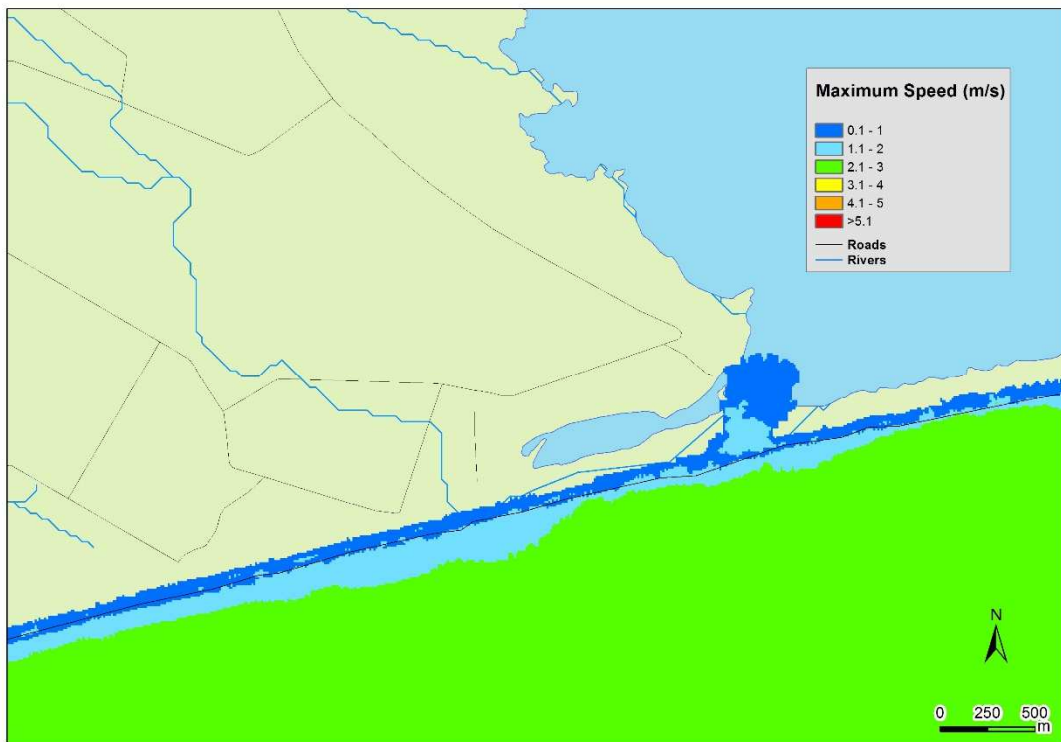
Figure 4-24: **Maximum flow speed for Taumutu village and the margins of Lake Ellesmere assuming the largest wave arrived at MHWS.**

4.2.12 Rakaia River Mouth (including north and south huts)

The maximum inundation depth and maximum flow speed for Rakaia River Mouth (including north and south huts) are shown in Figure 4-25 and Figure 4-26 respectively. The gravel barrier protecting the lagoon is inundated to over 2.5 m. All the edges of the lagoon are inundated including the seaward part of North Rakaia Huts. Water in the Rakaia River (not taken into account in our modelling) could allow surges to travel further up-river. Flow speeds reach up to 4 m/s in places overtopping the coastal dunes.
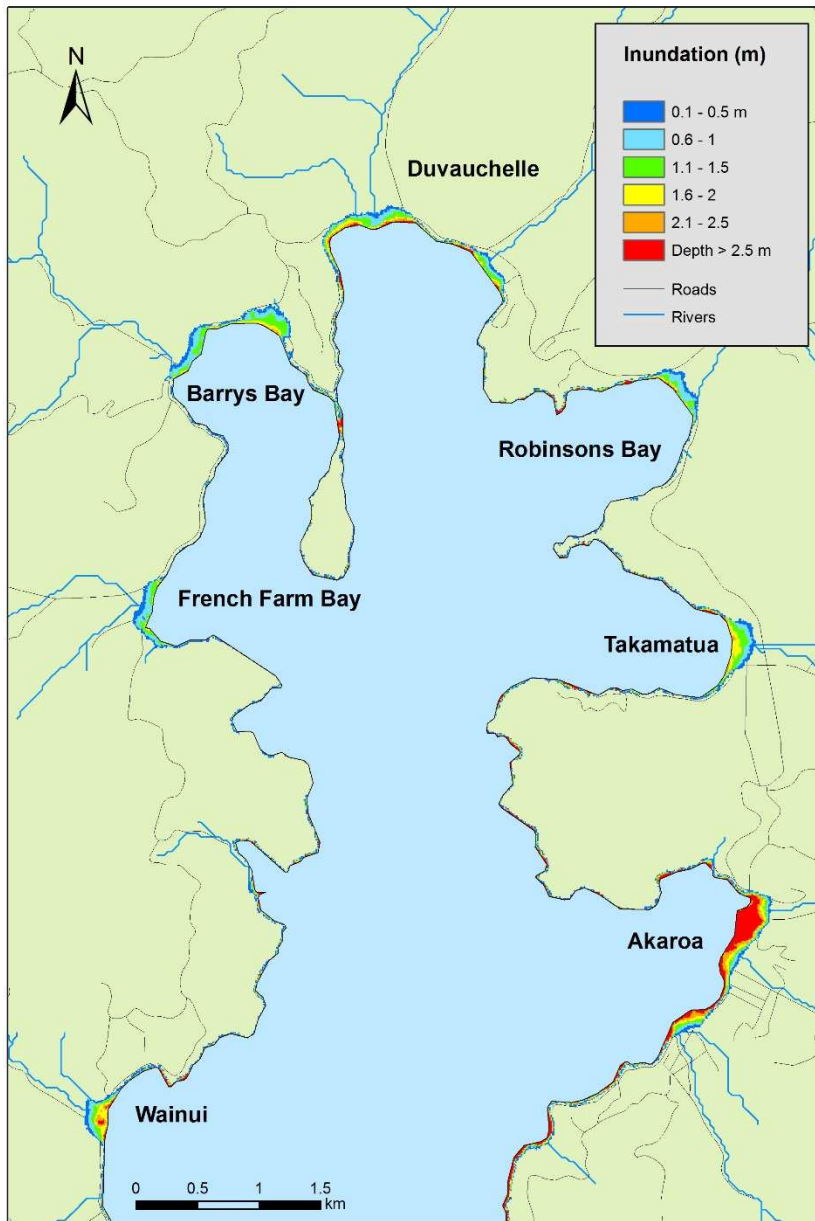

Figure 4-25:   Maximum inundation depth for the Rakaia River Mouth assuming the largest wave arrived at MHWS.   Inundation depths are only shown for inundated land.
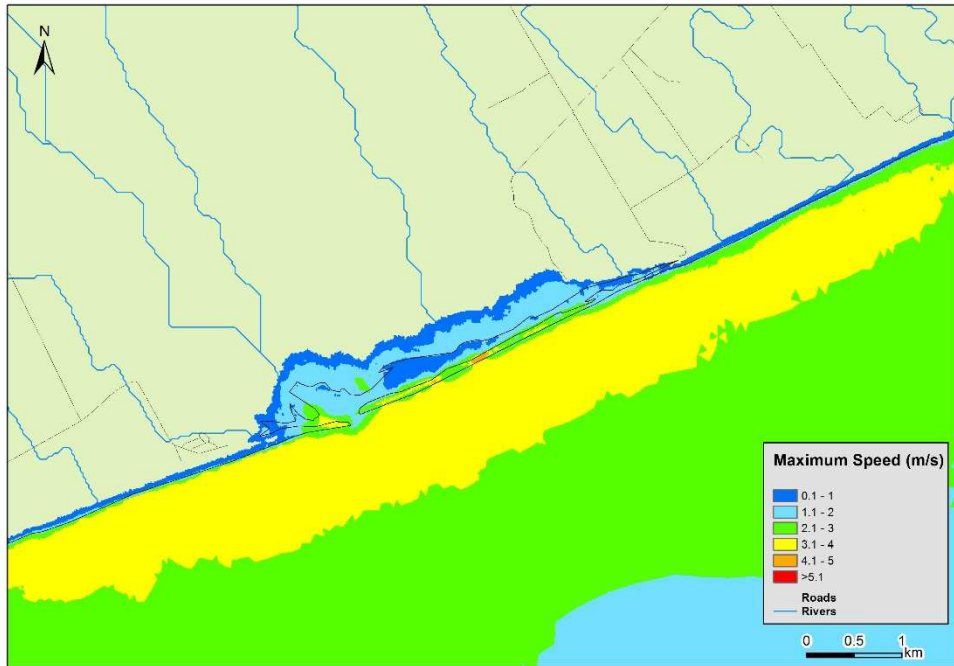
Figure 4-26:   Maximum flow speed for the Rakaia River mouth assuming the largest wave arrived at MHWS.

4.2.13 Rangitata River Mouth (including north and south huts)

Figure 4-27 and Figure 4-28 show the maximum inundation depth and maximum flow speed respectively for the Rangitata River Mouth assuming that the largest wave arrives at MHWS. There is inundation of the river mouth that will encompass some of the fishing huts on the northern bank of the Rangitata. Inundation gets close to the camping ground on the southern side of the river. Much of the flow reaches 3 m/s near the river mouth and some exceeds 4 m/s while overtopping the dunes. Water in the Rangitata River (not taken into account in our modelling) could allow surges to travel further up-river than shown in this modelling.
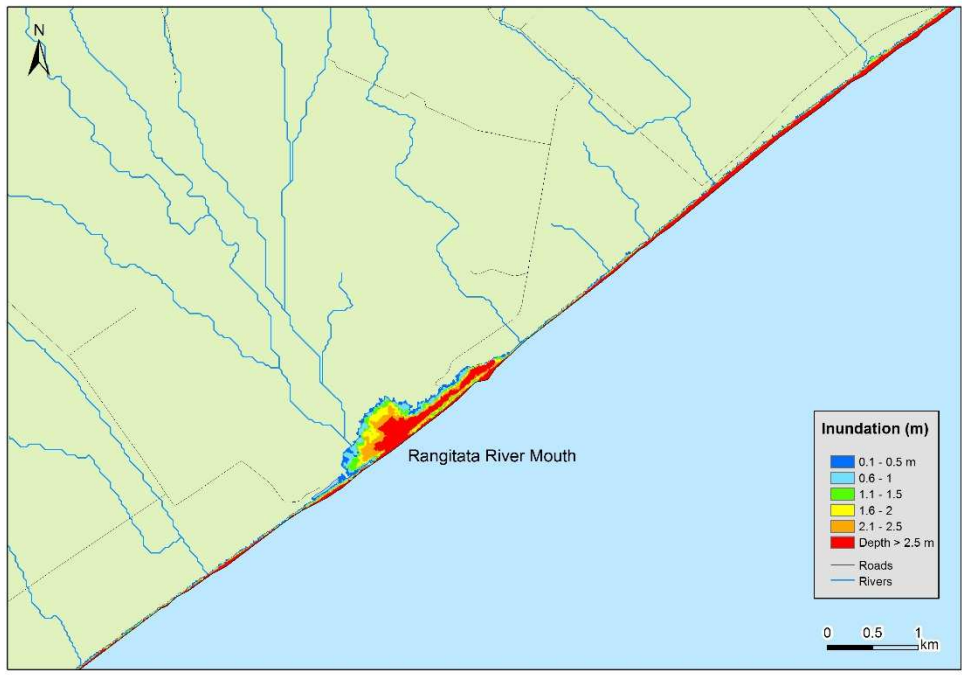
Figure 4-27: **Maximum inundation depth for the Rangitata River Mouth assuming the largest wave arrived at MHWS.** Inundation depths are only shown for inundated land.
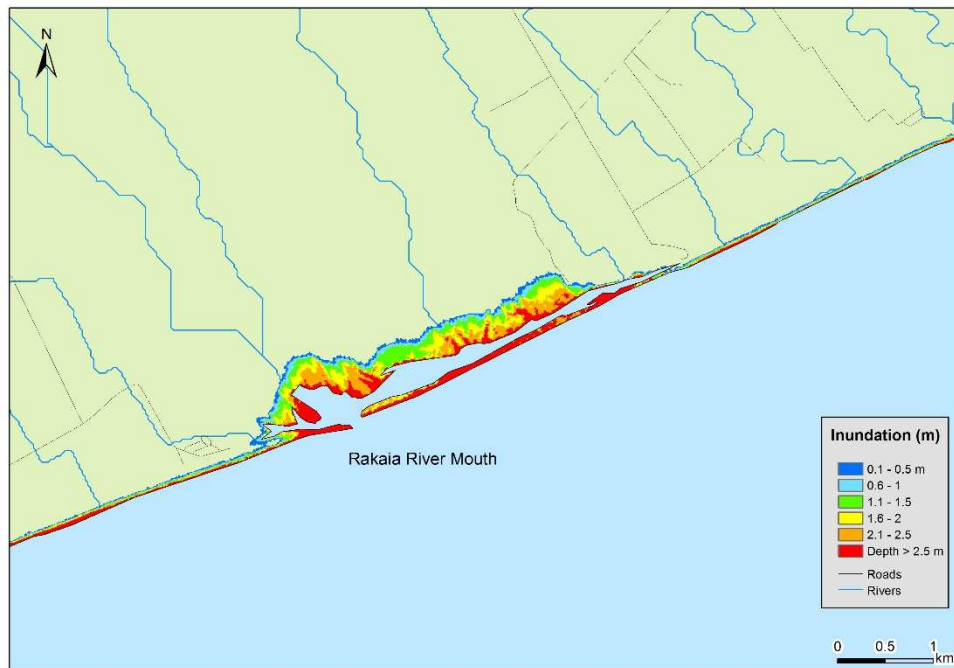

Figure 4-28: **Maximum flow speed for the Rangitata River Mouth assuming the largest wave arrived at MHWS.**

4.2.14 Browns Beach (Orari River Mouth to Opihi River Mouth and Waipopo)

Figure 4-29 and Figure 4-30 show the maximum inundation depth and maximum flow speed for Browns Beach assuming that the largest wave arrives at MHWS. The beachfront is inundated to over 2.5 m. Inundation also travels about 500 m up the Orari River and one kilometre up the Opihi River

and the surrounding land. Water in these rivers many also cause surges to be able to travel further upstream but this is not modelled in these simulations. Flow speeds reach over 2 m/s offshore of Browns Beach and up to 3 m/s at the mouth of the Opihi River. Note that although the stop banks around Milford Huts are not explicitly resolved in the inundation grid what is there from the LiDAR derived topography does stop the inundation of Milford Huts. If the stopbanks were explicitly resolved they might be higher than they are in this inundation grid but they would not be lower.

Figure 4-29:   Maximum inundation depth for Browns Beach assuming the largest wave arrived at MHWS. Inundation depths are only shown for inundated land.
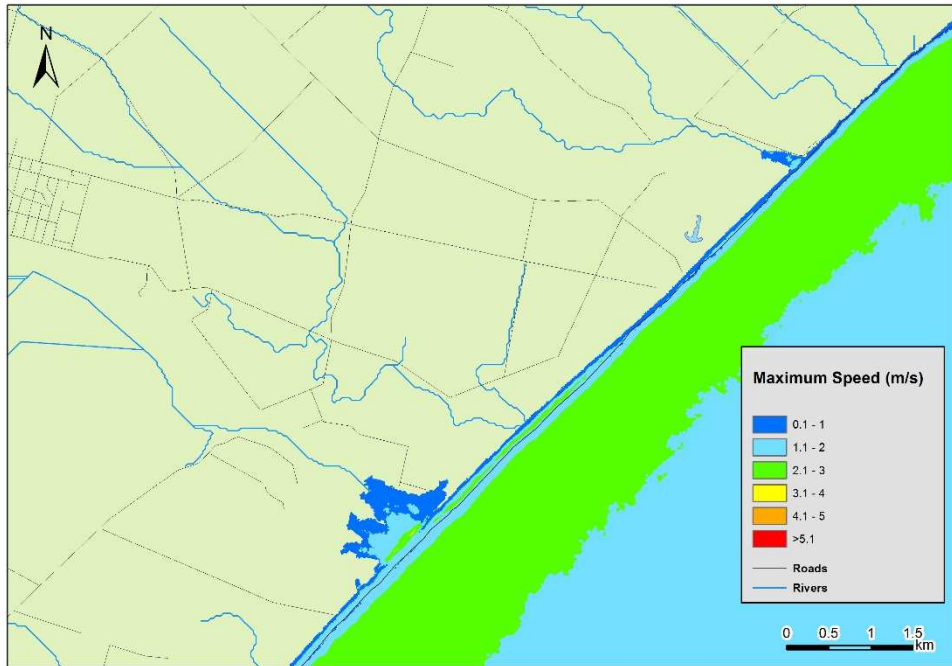
Figure 4-30:   Maximum flow speed for Browns Beach assuming the largest wave arrived at MHWS.

4.2.15 Seaforth to Scarborough (including Washdyke, Timaru, Saltwater Creek)

Figure 4-31 and Figure 4-32 show the maximum inundation depth and maximum flow speed respectively for Seaforth to Scarborough assuming that the largest wave arrives at MHWS. The flats north of Timaru are inundated 500-700 m inland in most places. Note though that coastal stop banks along this area are not explicitly included in the inundation grid. As can be seen in Figure 4-31 and Figure 4-32 they are there (inundation heights are lower in their vicinity and there is a speed up of the water flowing down the back of them) but depending on the placement of the grid it may not represent their maximum height. The explicit inclusion of the stop banks might reduce the amount of inundation in these areas. Caroline Bay and the Timaru Port are also inundated. Flow speeds are generally up to 2 m/s and can be in excess of 5 m/s in some places, especially around the port.

Figure 4-31: Maximum inundation depth for Seaforth to Scarborough assuming the largest wave arrived at MHWS. Inundation depths are only shown for inundated land.
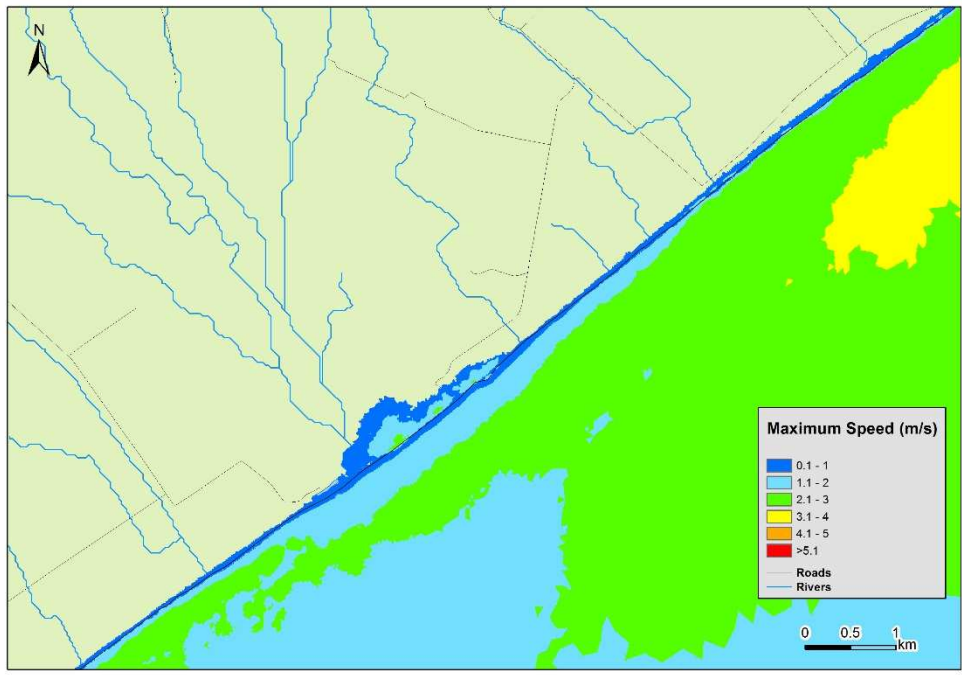
Figure 4-32: Maximum flow speed for Seaforth to Scarborough assuming the largest wave arrived at MHWS.

4.2.16 Pareora River Mouth (including Pareora Village and freezing works)

Figure 4-33 and Figure 4-34 show the maximum inundation depth and maximum flow speed respectively for Pareora River Mouth assuming that the largest wave arrives at MHWS. Inundation is mainly confined to the coastal strip going slightly further inland at the river mouth. Inundation gets close to the coastal road but does not cross it and so does not reach the freezing works. Flow speeds are over 2 m/s offshore. Water in the Pareora River (not taken into account in our modelling) could allow surges to travel further up-river than shown in this modelling.
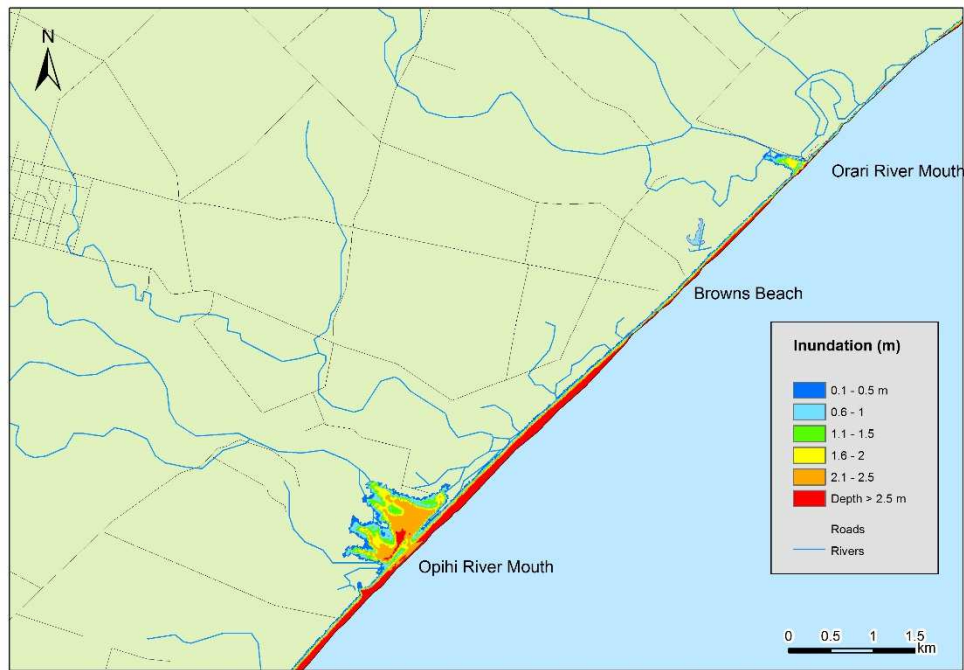
Figure 4-33:   Maximum inundation depth for Pareora River mouth assuming the largest wave arrived at MHWS.   Inundation depths are only shown for inundated land.
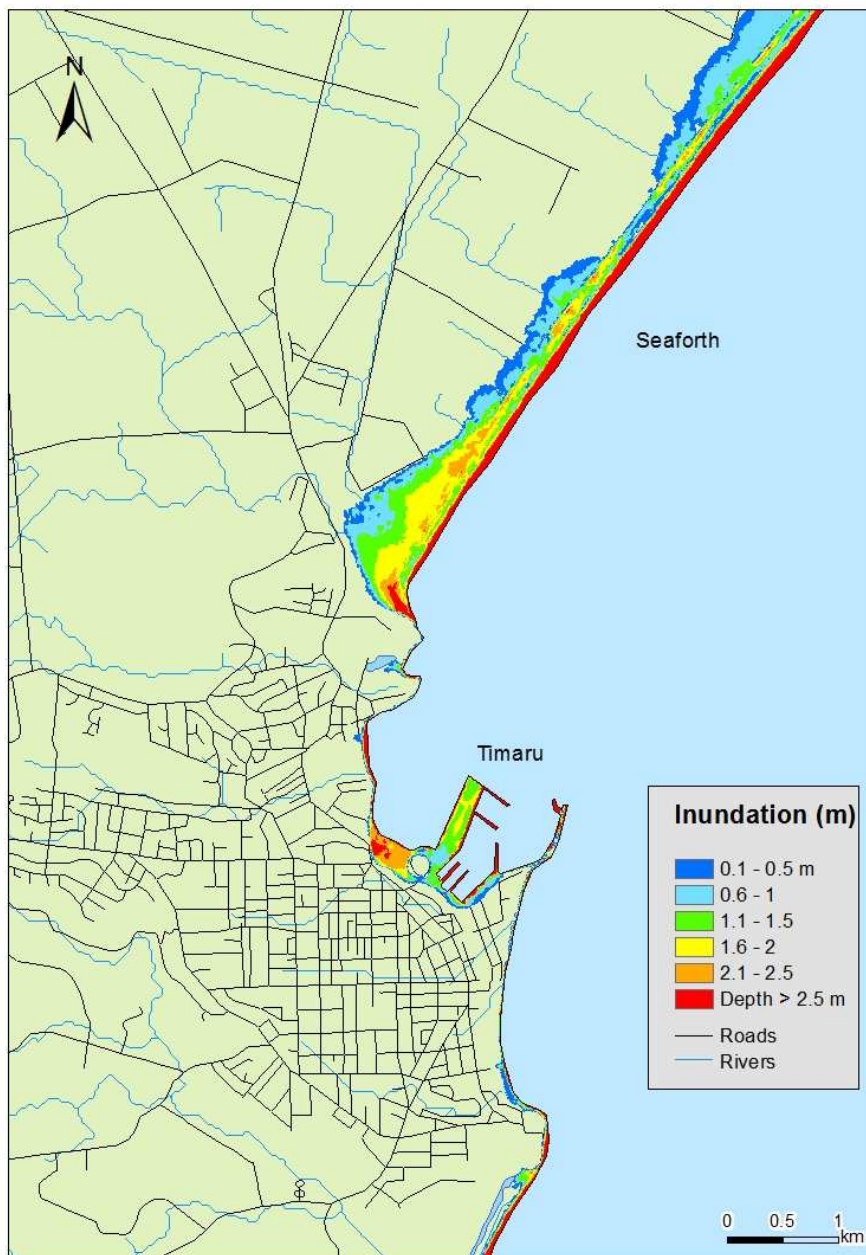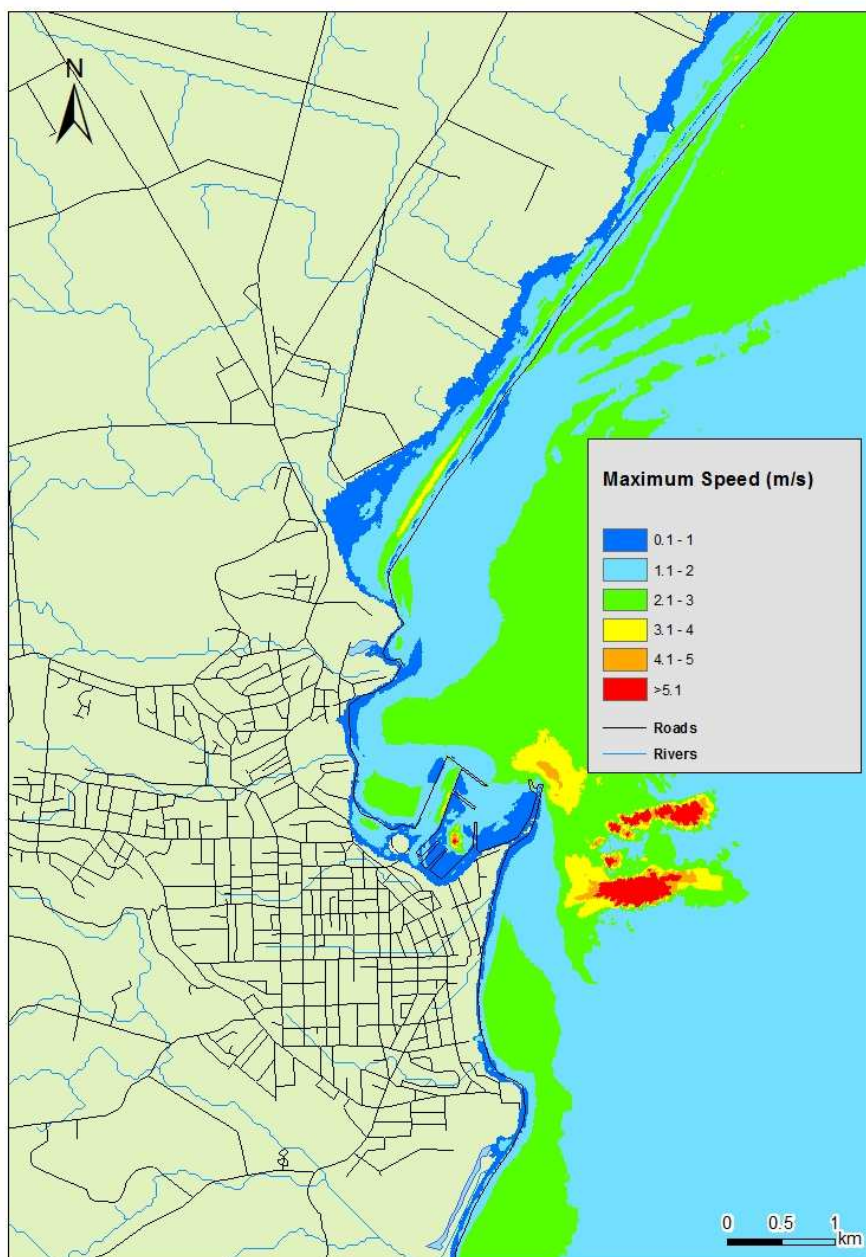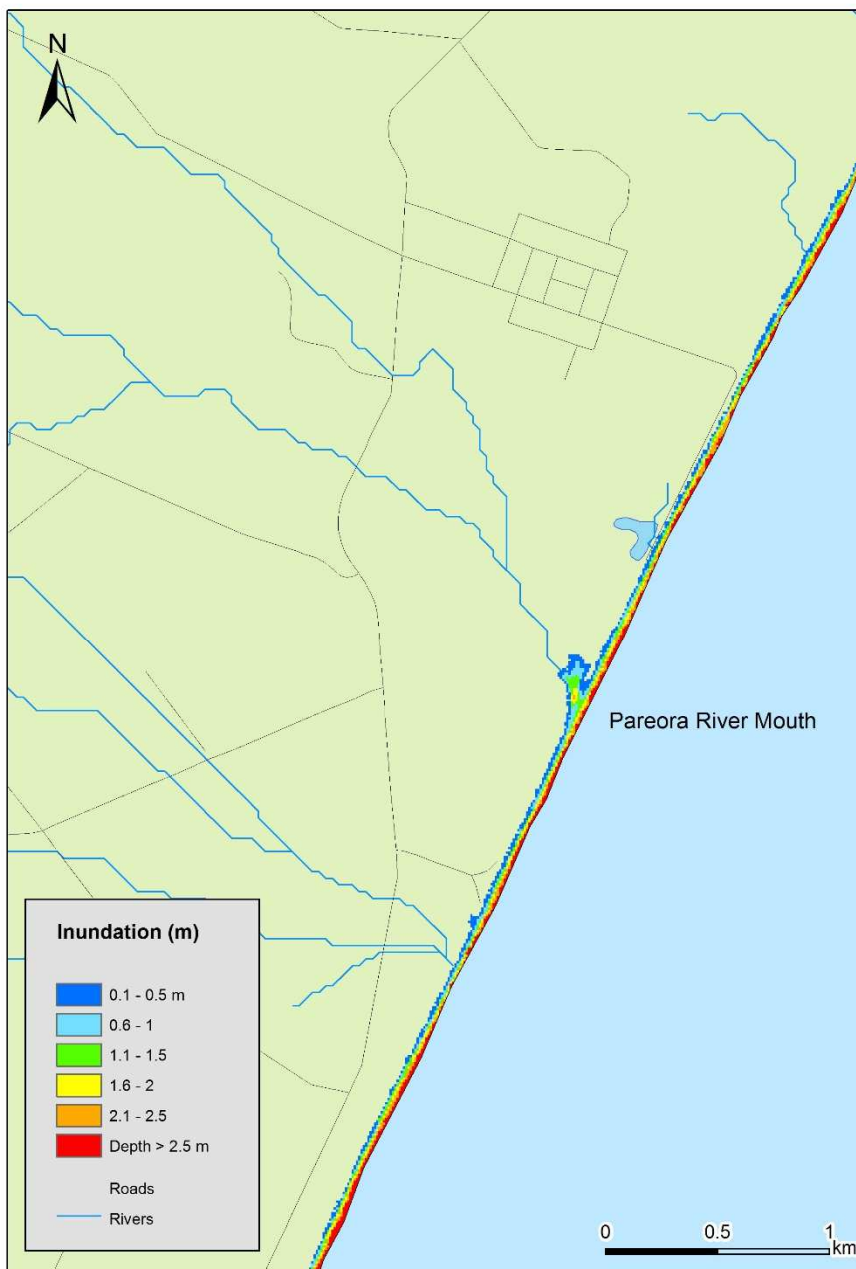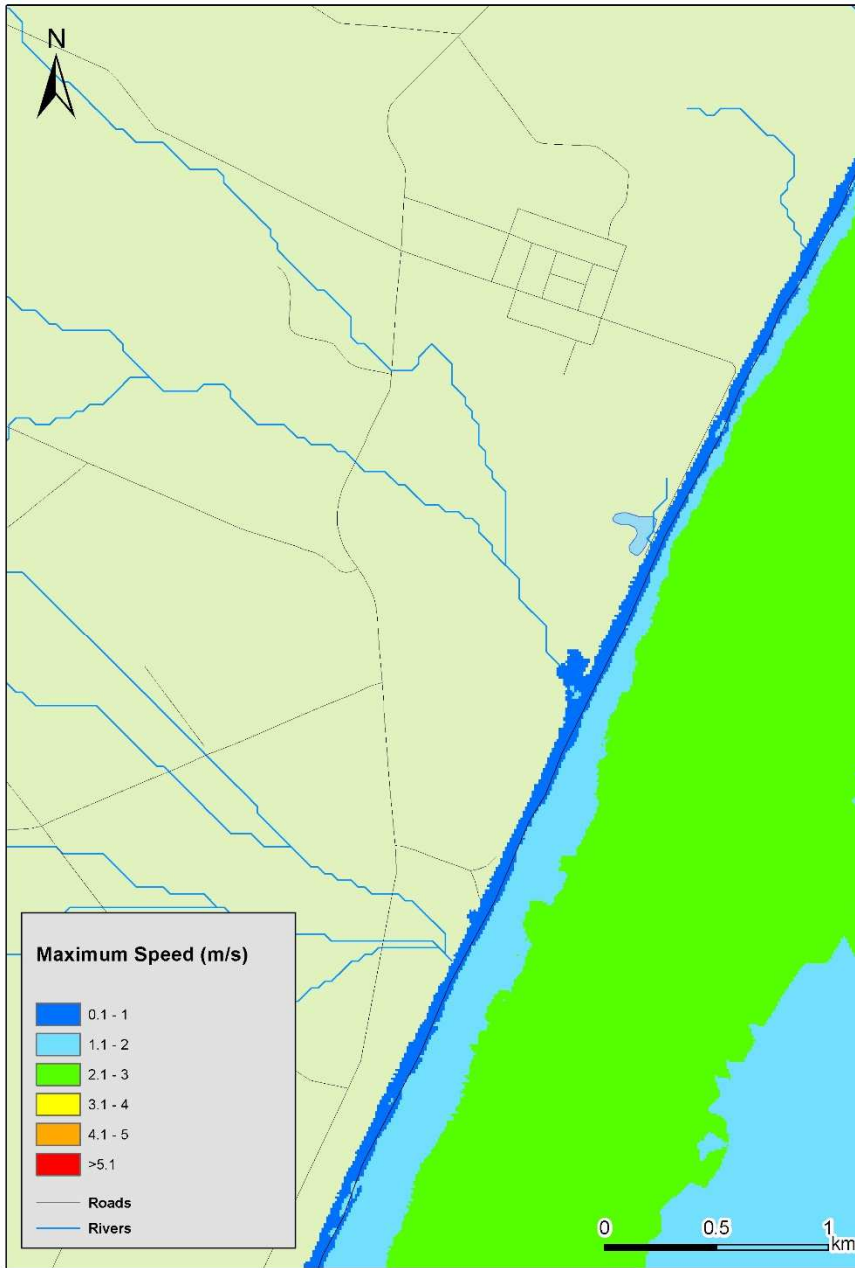
Figure 4-34:   Maximum flow speed for Pareora River mouth assuming the largest wave arrived at MHWS.

5   Conclusion

The South American tsunami modelled here causes significant coastal inundation in much of the Canterbury region. Largest wave heights are in Pegasus Bay and the bays on the northern side of Banks Peninsula where they exceed 10 m above the expected sea level in places and are over 8 m above the initial level in most of Pegasus Bay. North of Pegasus Bay the wave heights are not as high but in some places like around Kaikoura they do reach over 5 m above initial level. South of Banks Peninsula maximum wave heights range between 4 and 6 m above initial level.

This tsunami scenario causes extensive flooding along the Canterbury coast. Christchurch and Lyttelton Harbour face the worst inundation. Many of the coastal suburbs in Christchurch (New Brighton, South Shore, Redcliffs, Moncks Bay, Sumner, and Taylors Mistake) are extensively inundated to over 2.5 m in many places. Much of the low lying land in Lyttelton Harbour is inundated including almost all of Lyttelton Port. Although not modelled at high resolution here, many of the bays in Banks Peninsula are likely to be severely inundated as can be seen by the maximum wave heights in these bays. Although wave heights are not as large in Akaroa Harbour there is still extensive inundation of the low lying land including the main road in Akaroa Township. State Highway 1 is overtopped in several places in the Kaikoura region especially between Goose Bay and Oaro and some roads on the north and south sides of Kaikoura Peninsula are also inundated. Timaru Port is also inundated.

Flows speeds are generally over 2 m/s near the shore and can exceed 5 m/s at many river mouths when overtopping dunes, especially in the Pegasus Bay area. Flow speeds are generally lower along open coasts, especially in the Kaikoura area. Note that the modelling here is at a resolution of around 15 m. As such it may not resolve all the complicated small scale currents that may occur in enclosed waters such as ports and marinas. As such, in ports and marinas, these numbers should be taken as a minimum.

This modelling assumes a fixed bathymetry and topography. Large tsunamis waves could considerably erode dunes and other structures that they overtop which could leave the land behind them open to attack by subsequent waves. Rivers are not explicitly modelled with water in these simulations. The water in rivers could cause tsunami surges to travel further upstream than shown in these simulation although it would not be expected to cause significant extra inundation.

Despite the inherent uncertainties in numerical modelling of tsunami impacts, we believe that the current modelling exercise provides the best estimate of distant-source tsunami-related inundation of Canterbury available to date.

6   References

Bell, R.G. (2011) Sumner Head Sea-level Station: Annual Report for 2009-2010. *NIWA Client Report*, HAM2011-051.

Berryman, K. (2005) Review of tsunami hazard and risk in New Zealand. *Institute of Geological & Nuclear Sciences client report* 2005/104: 139.

Cox, R.J., Shand, T.D., Blacka, M.J. (2010) Australian Rainfall and Runoff Revision Project 10: Appropriate Safety Criteria for People. *Australian Rainfall and Runoff Report Number P10/S1/006*: 31.

Delouis, B., Pardo, M., Legrand, D., Monfret, T. (2009) The M-w 7.7 Tocopilla Earthquake of 14 November 2007 at the Southern Edge of the Northern Chile Seismic Gap: Rupture in the Deep Part of the Coupled Plate Interface. *Bulletin of the Seismological Society of America*, 99(1): 87-94. 10.1785/0120080192

Downes, G. (2013) New Zealand historical tsunami database. GNS Science.

GEBCO (2013) General Bathymetric Chart of the Oceans (GEBCO). http://www.gebco.net/

Gillibrand, P.A., Arnold, J., Lane, E.M., Roulston, H., Enright, M. (2011) Modelling Coastal Inundation in Canterbury from a South American Tsunami. *NIWA Client Report*, CHC2011-009: 55 p.

Gillibrand, P.A., Power, W.L., Lane, E.M., Wang, X., Sykes, J.R.E., Brackley, H., Arnold, J. (2010) Probabilistic hazard analysis and modelling of Tsunami inundation for the Auckland region from regional source Tsunami. *NIWA Client Report*: 62 p. : ill., maps, tables, refs p. 54-56. Q:\Library\Originals\Client Reps\2010

Goff, J., Chague-Goff, C. (2012) A review of palaeo-tsunamis for the Christchurch region, New Zealand. *Quaternary Science Reviews*, 57: 136-156. 10.1016/j.quascirev.2012.10.004

Goff, J.R., Lane, E.M., Arnold, J.R. (2009) The tsunami geomorphology of coastal dunes. *Natural Hazards and Earth System Sciences*, 9(3): 847-854. <Go to ISI>://WOS:000267543300017

Goff, J.R., Nichol, S., Chague-Goff, C., Horrocks, M., McFadgen, B., Cisternas, M. (2010) Predecessor to New Zealand's largest historic trans-South Pacific tsunami of 1868 AD. *Marine Geology*, 275(1-4): 155-165. 10.1016/j.margeo.2010.05.006

Goring, D.G. (2010) MHWS at Kaikoura.

Henry, R.F., Walters, R.A. (1993) Geometrically-based, automatic generator for irregular triangular networks. *Communications in Numerical Methods in Engineering*, 9(7)(555-566).

HR Wallingford (2006) Flood risks to people. *Defra /Environment Agency Flood and Coastal Defence R&D Programme. *, FD2321/TR2 Guidance Document: 91. http://www.rpaltd.co.uk/documents/J429-RiskstoPeoplePh2-Guidance.pdf

Lane, E.M., Arnold, J.R. (2013) Tsunami inundation modelling for Kaikoura and North Canterbury. *NIWA Client Report*, CHC2013-124 34 p.

Lane, E.M., Arnold, J., Sykes, J., Roulston, H. (2012) Modelling coastal inundation in Christchurch and Kaiapoi from a South American tsunami using topography from after the 2011 February earthquake. *NIWA Client Report*, CHC2011-129 36 p.

Lane, E.M., Gillibrand, P.A., Arnold, J.R., Walters, R.A. (2011) Tsunami inundation modelling using RiCOM. *Australian Journal of Civil Engineering*, 9(1): 83-98.

Lane, E.M., Walters, R.A., Arnold, J.R., Enright, M., Roulston, H. (2007a) Auckland Regional Council Tsunami Inundation Study. *NIWA Client Report*, CHC2007-126.

Lane, E.M., Walters, R.A., Wild, M., Arnold, J., Enright, M., Roulston, H., Mountjoy, J. (2007b) Otago region hazards management investigation: tsunami modelling study. *NIWA Client Report*, CHC2007-030: 253.

LINZ (2010) Sea Level Data. Land Information New Zealand. http://www.linz.govt.nz/hydro/tidal-info/gauges

New Zealand Nautical Almanac (NZ204) (2012) *New Zealand Nautical Almanac* Marine Division, Wellington. http://www.linz.govt.nz/hydro/nautical-info/about-nz-almanac

Pederson, G. (2008) Modeling runup with depth integrated equation models. In: P.L.-F. Liu, H. Yeh & C. Synolakis (Eds). *Advances in coastal and ocean engineering: Advanced numerical models for simulating tsunami waves and runup*. World Scientific: 3-41.

Power, W.L. (2013a) Review of Tsunami Hazard in New Zealand (2013 Update), GNS Science Consultancy Report 2013/131.

Power, W.L. (2013b) Tsunami hazard curves and deaggregation plots for 20km coastal sections, derived from the 2013 Nation Tsunami Hazard Model. *GNS Science Report* GNS Science Report 2013/59.

Ramirez-Herrera, M.T., Cundy, A., Kostoglodov, V., Carranza-Edwards, A., Morales, E., Metcalfe, S. (2007) Sedimentary record of late-Holocene relative sea-level change and tectonic deformation from the Guerrero Seismic Gap, Mexican Pacific Coast. *Holocene*, 17(8): 1211-1220. 10.1177/0959683607085127

Staniforth, A., Coté, J. (1991) Semi-Lagrangian integration schemes for atmospheric models - a review. *Monthly Weather Review*, 119(9): 2206-2223.

Swenson, J.L., Beck, S.L. (1996) Historical 1942 Ecuador and 1942 Peru subduction earthquakes, and earthquake cycles along Colombia Ecuador and Peru subduction segments. *Pure and Applied Geophysics*, 146(1): 67-101. <Go to ISI>://WOS:A1996TX02400005

Wallace, L.M., Reyners, M., Cochran, U., Bannister, S., Barnes, P.M., Berryman, K., Downes, G., Eberhart-Phillips, D., Fagereng, A., Ellis, S., Nicol, A., McCaffrey, R., Beavan, R.J., Henrys, S., Sutherland, R., Barker, D.H.N., Litchfield, N., Townend, J., Robinson, R., Bell,

R., Wilson, K., Power, W. (2009) Characterizing the seismogenic zone of a major plate boundary subduction thrust: Hikurangi Margin, New Zealand. *Geochemistry Geophysics Geosystems*, 10. 10.1029/2009gc002610

Walters, R.A. (2005a) Coastal ocean models: two useful finite element methods. *Continental Shelf Research*, 25(7-8): 775-793. 10.1016/j.csr.2004.09.020

Walters, R.A. (2005b) A semi-implicit finite element model for non-hydrostatic (dispersive) surface waves. *International Journal for Numerical Methods in Fluids*, 49(7): 721-737. 10.1002/fld.1019

Walters, R.A., Barnes, P., Goff, J.R. (2006a) Locally generated tsunami along the Kaikoura coastal margin: Part 1. Fault ruptures. *New Zealand Journal of Marine and Freshwater Research*, 40(1): 1-16. <Go to ISI>://WOS:000237691000001

Walters, R.A., Barnes, P., Lewis, K., Goff, J.R. (2006b) Locally generated tsunami along the Kaikoura coastal margin: Part 2. Submarine landslides. *New Zealand Journal of Marine and Freshwater Research*, 40(1): 17-28. <Go to ISI>://WOS:000237691000002

Walters, R.A., Barnes, P., Lewis, K., Wild, M., Duncan, M.J., Shankar, U., Goff, J.R. (2003) Kaikoura District engineering lifelines project : tsunami hazard assessment (Part 1). *NIWA Client Report*, CHC2003-033: 155.

Walters, R.A., Casulli, V. (1998a) A robust, finite element model for hydrostatic surface water flows. *Communications in Numerical Methods in Engineering*, 14(10): 931-940. 10.1002/(sici)1099-0887(1998100)14:10<931::aid-cnm199>3.0.co;2-x

Walters, R.A., Casulli, V. (1998b) A robust, finite element model for hydrostatic surface water flows. *Communications in Numerical Methods in Engineering*, 14: 931-940.

Walters, R.A., Goff, J.R., Wang, K. (2006) Tsunamigenic sources in the Bay of Plenty, New Zealand. . *Science of Tsunami Hazards*, 24: 339-350.

Walters, R.A., Lane, E.M., Hanert, E. (2009) Useful time-stepping methods for the Coriolis term in a shallow water model. *Ocean Modelling*, 28(1-3): 66-74. 10.1016/j.ocemod.2008.10.004

Walters, R.A., Lane, E.M., Henry, R.F. (2007) Semi-Lagrangian methods for a finite element coastal ocean model. *Ocean Modelling*, 19(3-4): 112-124. 10.1016/j.ocemod.2007.06.008

Appendix A   GIS layers

The GIS rasters for Figure 4-3 through Figure 4-34 are included in the CD in the case at the back of this report. The spatial data in these layers have been generated at a scale of 1:25,000 and should not be used at scales finer than this.

Appendix B   Tsunami related websites

New Zealand Websites

NIWA tsunami web page

https://www.niwa.co.nz/natural-hazards/hazards/tsunami

Geonet tsunami gauges

http://www.geonet.org.nz/tsunami/

NIWA sea level page

https://www.niwa.co.nz/our-science/coasts/tools-and-resources/sea-levels

Overseas web sites

Natural Hazards Data, Images and Education, National Geophysical Centre, National Oceanic and Atmospheric Administration (NOAA)

http://tsunami.noaa.gov/

http://www.ngdc.noaa.gov/hazard/tsu_travel_time.shtml

http://www.coastal.jp/tsunami2011/

UNESCO information about tsunami

http://www.ioc-tsunami.org/

http://itic.ioc-unesco.org/index.php

http://itic.ioc-unesco.org/images/stories/about_tsunamis/tsunami_glossary/tsunami_glossary_en_2013_web.pdf

http://itic.ioc-unesco.org/index.php?option=com_content&view=category&layout=blog&id=2000&Itemid=2000&lang=en

Tsunami warnings and alerts for the Pacific.

http://ptwc.weather.gov/?region=1